UNIVERSITEIT
GENT

Report AquaSPICE

Case study at BASF Antwerp
Part III: Wastewater treatment plant effluent reuse

BASF
We create chemistry

evides
industriewater

The Improved containers on site at BASF Antwerp

Case study WWTP BASF Antwerp: test period July 10 – Oct 1 2024

Main authors
Ivaylo Hitsov, PhD, *UGent* (Preparation of the report, operator)
Valeriy Matveev, MSc, *UGent* (Preparation of the report, operator)
Evgeniy Matveev, MSc, *UGent* (Preparation of the report, operator)

Correctors
Kristof de Neve, PhD, *BASF,* project supervision and support
Lisa Wyseure, MSc, *Evides Industriewater*

Others involved
Joachim Wauman, MSc, *BASF,* project supervision and support
Peter J. Verheyden, BSc, *BASF,* operational support and project organization
Matthias Materne, MSc, *BASF,* Lab analyses
Dirk Rens, MSc, *BASF,* Lab analyses
BASF control room operators and engineers
David Moed, PhD, *Evides Industriewater,* project supervision and technical advice
Jaap Regelink, MSc, *Evides Industriewater,* technical advice
Mark Boers, MSc, *Evides Industriewater,* technical advice

Contents

1. Abstract

During the third part of the AquaSPICE trials at BASF, the IMPROVED containers were deployed at the wastewater treatment plant of BASF. The flowrate on average was 1300 m^3/h with conductivity of 12-15 mS/cm and total organic carbon (TOC) of 15-40 ppm. The effluent coming from one of the five settlers was fed to the pilots where it was pretreated using ultrafiltration and recovered using Revere Osmosis (RO) and Closed Circuit Reverse Osmosis CCRO. In this feasibility test the aim was to reuse the water to process water (<700 µS/cm and < 5ppm TOC) or better standards. Also, a comparison between the RO and CCRO was made to evaluate operational issues, advantages and disadvantages of the two technologies. The CCRO inside the IMPROVED containers has been converted in SITU and is not an official DuPont installation. That being said, a permission from DuPont was asked before this mimic CCRO configuration was done.

The tests showed that the water quality produced by the RO and CCRO was sufficient to be reused as process water since the conductivity of the RO permeate was 300-800 µS/cm. More importantly, the TOC produced was less than 1ppm which suggests that the water could even be fed to the demin plant to produce boiler feed water. The current source of boiler feed water at BASF has TOC levels of 2-4 ppm TOC. In terms of operational stability, the WWTP effluent was very challenging for the UF and it had to be operated at flux of around 25 Lmh in order to achieve a stable operation. The water was also very challenging for the conventional RO since the membrane became irreversibly fouled after only 20 days and the fouling was completely irreversible after cleaning with acids, bases, chelating agents and non-ionic surfactants. On the other hand the CCRO performed much better and the membrane performed well for 5 weeks with the fouling tendency appearing to reach a plateau. Both the RO and the CCRO were operated at 17 Lmh flux and 66 % recovery.

2. Introduction

Access to fresh water is crucial for the chemical industry, as it is essential for various processes, including water treatment at wastewater treatment plants (WWTPs). However, the consistent supply of fresh water is increasingly at risk due to the increasing scarcity and declining quality of both ground and surface water sources, with rising salinity levels being a significant concern. The Biesbosch water that is used as the main water source of BASF is also used for drinking water production and farming irrigation, placing BASF in a vulnerable position in draught periods. To address these challenges, implementing sustainable practices such as recycling industrial process water and utilizing alternative water sources becomes imperative.

Within the trials the possibility to reuse the wastewater treatment plant effluent was studied. The aim was to reuse the water as process water (< 800 µS/cm and < 5ppm TOC). For this, the IMPROVED water treatment containerized pilots were used. These pilots were built within the IMPROVED project funded by Interreg Flanders-Netherlands. The IMPROVED pilots are housed in two 40 ft sea shipping containers and contain nine water treatment skids that can be rearranged in different configurations. They can treat up to two streams at the same time with nominal flow rate of 250 l/h each. The available water treatment skids are Reverse Osmosis (RO), Ultrafiltration (UF), Ion Exchange (IEX), Granular Activated Carbon (GAC), Electrodeionization (EDI), Electrodialysis with reversal possibility (EDR), Advanced Oxidation Processes (AOP), Membrane Aerated Bioreactor (MABR), and coagulation and flocculation including a lamella settler.

2.1 Problem Statement of the BASF Antwerp Case

BASF holds the title of the world's leading manufacturer of basic chemicals. Its facility in Antwerp ranks as the second largest BASF site and relies on Biesbosch surface water for producing demineralized water and process water.

The BASF Antwerp wastewater treatment plant (WWTP) operates a comprehensive system for wastewater treatment that includes physical-chemical, mechanical, and biological treatment stages. The treatment process consists of the following main components:

1. **Neutralization**: Wastewater with varying acidity levels is collected and mixed, where partial neutralization and buffering occur. Adjustments to pH levels (if outside the range of 7.0 to 7.5) are made using sodium hydroxide, sodium carbonate, or sulfuric acid.
2. **Sand Trap**: Before reaching the aeration basins, the wastewater passes through sand trap to remove coarse, settleable materials, which helps prevent equipment wear and reduces sediment build-up.
3. **Aeration Basins**: These basins, organized as three elongated carousels, handle the biological treatment. Wastewater is introduced into the first basin, where anoxic pre-denitrification sections reduce nitrate levels. The basins have zones for oxygen dosing, where organic materials are broken down into CO2 and biomass, and nitrification, converting ammonia nitrogen to nitrate and nitrite. A low-oxygen area facilitates denitrification, converting nitrates and nitrites to nitrogen gas.
4. **Settling Basins**: The mixture of sludge and water is directed to settling basins, where sludge is separated from the treated water, the latter is then discharged into the Scheldt River. Most of the sludge is returned to the aeration basins, maintaining microbial activity for effective treatment.
5. **Ozonation**: Some sludge is treated with ozone in a dedicated reactor, using ozone generated on-site. This treatment aims to adapt the settling properties of the sludge and to reduce the sludge volume production
6. **Thickeners and Decanters**: A portion of the sludge is directed to thickeners and decanters for further water removal, after which the dewatered sludge is incinerated externally with energy recovery.

The WWTP operates under continuous monitoring to ensure compliance with discharge standards, particularly for parameters like Biological Oxygen Demand (BOD), Chemical Oxygen Demand (COD), and nitrogen compounds. The treatment plant is managed by the BASF Energy/WWTP service, which oversees capacity and load assessments, ensuring that the plant can handle variable wastewater inputs while minimizing environmental impacts.

With the AquaSPICE project, the BASF Antwerp plant strives to investigate and increase knowledge of cost-effective treatments for water reuse, concerning:

a) The reuse of RO concentrate from the new demineralized water production plant.

b) The reuse of process condensate streams and process streams from the steam cracker plant for direct reuse or reuse after treatment.

c) Reuse its wastewater treatment plant effluent for production of demineralized or process water (current report)

2.2 Goal

The schematic representation of the technologies tested at the WWTP of BASF Antwerp can be seen in Figure 1:

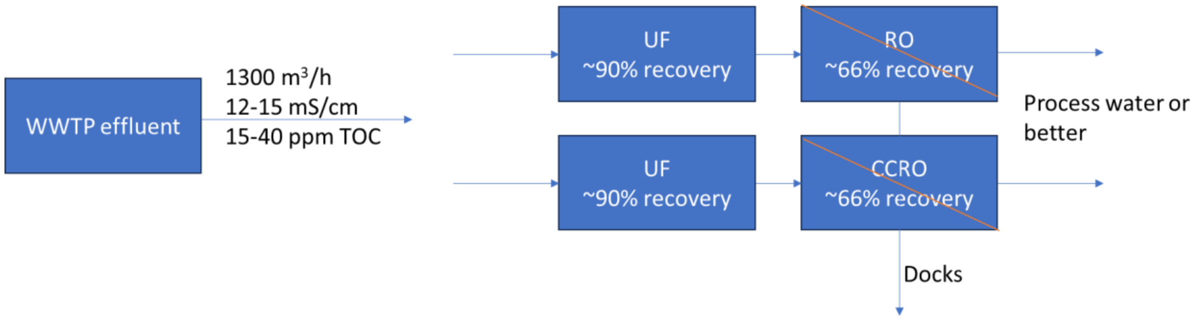

Figure 1 Schematic representation of the technologies tested at the WWTP of BASF Antwerpen

3. Technologies of interest – theoretical background

Reverse osmosis

In RO, a pressure gradient leads to separation through a semipermeable membrane. The RO membranes typically do not have visible pores and are considered dense membranes. The suspended solids are mechanically rejected by the membrane, while salts and water are dissolved into the active layer and the rejection is dictated by difference in diffusion coefficients of the water and solutes. Other factors such as membrane and solute charge also have a significant role in the determination of the rejection, but this is out of the scope of this report.

Salts, suspended solids, viruses, and dissolved components are retained in the concentrate, while water and some limited dissolved components move through the membrane in the permeate. RO membranes are typically not cleaned by backwashing but are mostly cleaned-in-place (CIP), or can be flushed with air to remove fouling and prevent clogging of the feed spacer.

Closed circuit reverse osmosis (CCRO)

The CCRO alternates between two modes of operation: closed-circuit desalination and flush cycle. In closed-circuit mode, the RO recirculates all of the concentrate stream blended with raw feed and produces no brine (Figure 2). The pressure increases subsequently as the concentation and the osmotic pressure in the loop increases. Once a setpoint is reached, the system transitions to plug-flow, the concentrate valve opens and the system is flushed. The continuous changing hydraulic and osmotic pressure conditions are unfavorable for microorganisms, and thereby reducing fouling. The purging of the brine, before crystals can form, avoids scaling. In addition, the water recovery of CCRO is higher than conventional RO, thereby decreasing the waste stream. But the permeate quality will fluctuate during the concentration cycle, requiring a permeate buffer tank [1] [2] [3] [4].

The CCRO was implemented by modifying the conventional RO in the containers in accordance with the patent holder DuPont who allowed the modification exceptionally for UGent. The concentrate stream was directed to the feed of the pump instead of the buffer tank and the programming was adjusted to accommodate the cyclic nature of CCRO. The water is recycled in the system for a set number of minutes and then the system is flushed with the calculated dead volume of the system. The ratio of the volumes produced in the filtration and flush cycle dictates the recovery of the system.

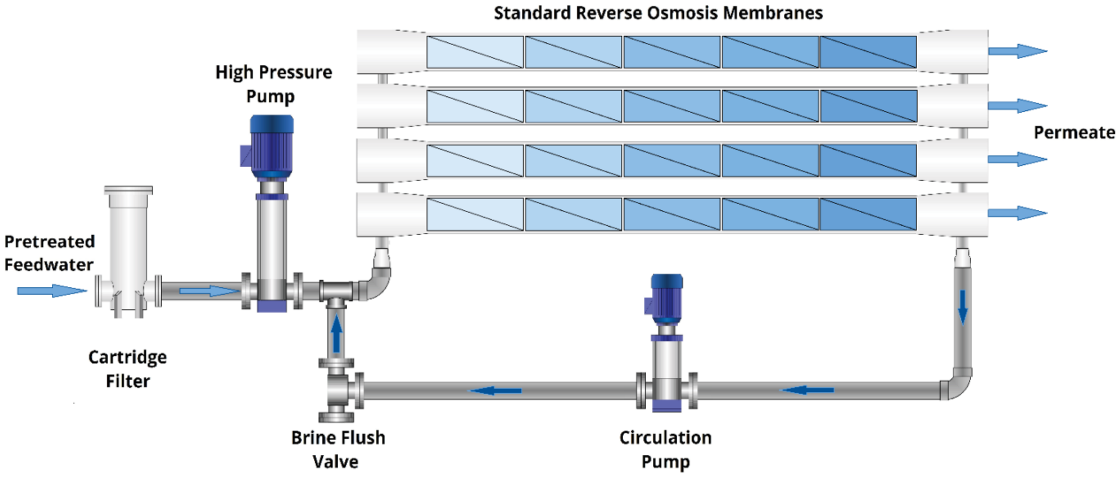

Figure 2 Schematic overview of the working principle of CCRO during closed circuit mode; after each filtration cycle the brine flush valve will open for certain amount of time [5]

Ultrafiltration

Ultrafiltration is a membrane-based separation process widely used in various industries, including water treatment, pharmaceuticals, and food processing. Fundamentally, ultrafiltration operates on the principle of size exclusion, where a semi-permeable membrane selectively allows smaller molecules and solvents to pass through while retaining larger solutes such as proteins, colloids, and suspended solids. The membranes used in ultrafiltration typically have pore sizes ranging from 1 to 100 nanometers, which are engineered to target specific contaminants based on their molecular weight. The driving force for the separation process is pressure, applied to facilitate the movement of the feed solution through the membrane.

The efficiency of ultrafiltration is influenced by several theoretical factors, including flux rate, rejection rate, and fouling propensity. Flux rate refers to the volume of liquid that can pass through the membrane per unit area and time, and it is a critical parameter for assessing the performance of the system. Higher fluxes allow for smaller membrane area to be utilized and therefore lower capex, but can lead to problems with fouling which may require more frequent membrane cleaning, shorter membrane lifetime and more equipment downtime. Rejection rate, on the other hand, measures the membrane's ability to retain specific solutes, ensuring the quality of the permeate. Fouling, the accumulation of unwanted materials on the membrane surface, poses a significant challenge as it can reduce permeability and necessitate regular cleaning or membrane replacement.

4. Materials and Methods

Reverse osmosis

In Figure 3 the scheme of the RO set-up is shown. The used RO membrane was a Dupont FilmTec BW30PRO 4040, with an active membrane area of and 7.9 m^2. The pressure housing was a Codeline 40E100. The pH of the feed water, flowrate of permeate and recycle, pressure of feed and concentrate, conductivity of feed, concentrate and permeate as well as feed temperature were continuously measured online with 10-seconds sampling intervals.

A general overview of the RO layout is provided in Figure 3.

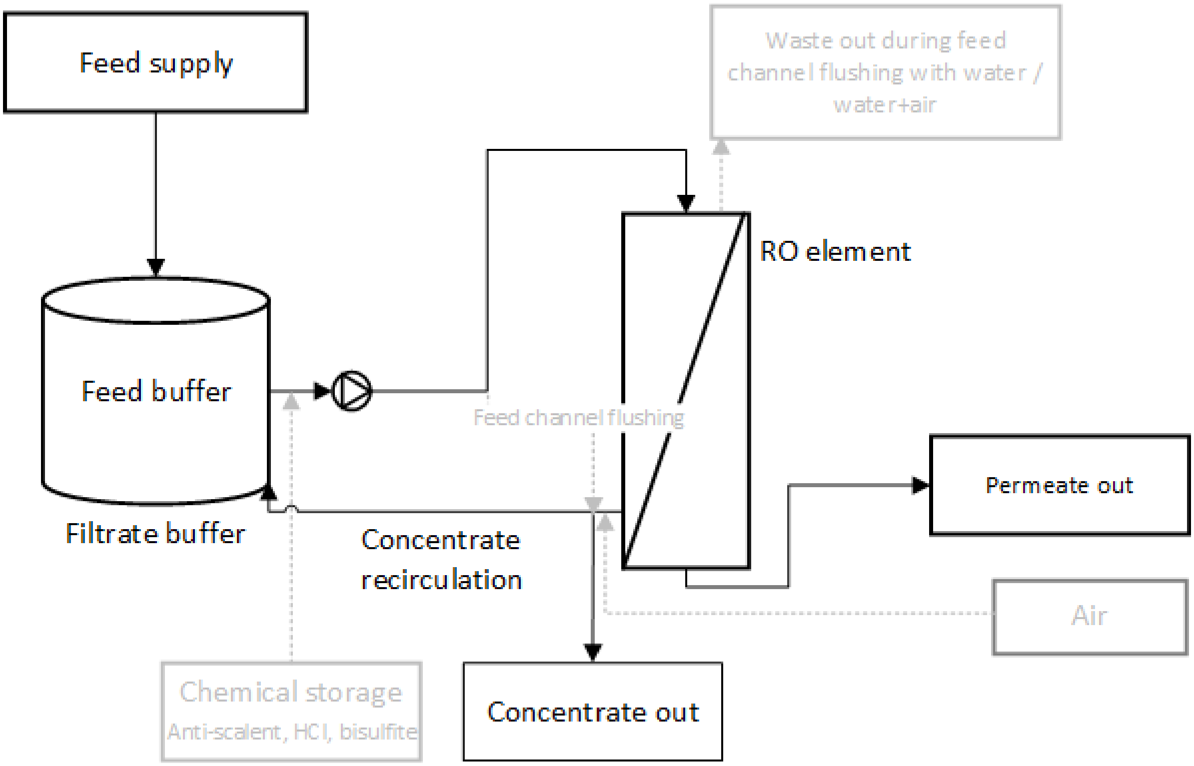

Figure 3 Schematic overview of the conventional RO module. The lines in gray are used only during cleaning in place or injection of air.

The RO was modified to CCRO by rerouting the concentrate recirculation to the suction of the high RO pump and by installing a brine discharge valve before the backpressure regulator that is located at the concentrate outlet of the pressure vessel.

Ultrafiltration

The ultrafiltration is a process where suspended solids are filtered over a membrane with small pores. This process is commonly used as a pretreatment process for reverse osmosis. The membranes used in UF can be backwashed periodically and are resistant to low levels of free chlorine allowing cleaning in place with bleach.

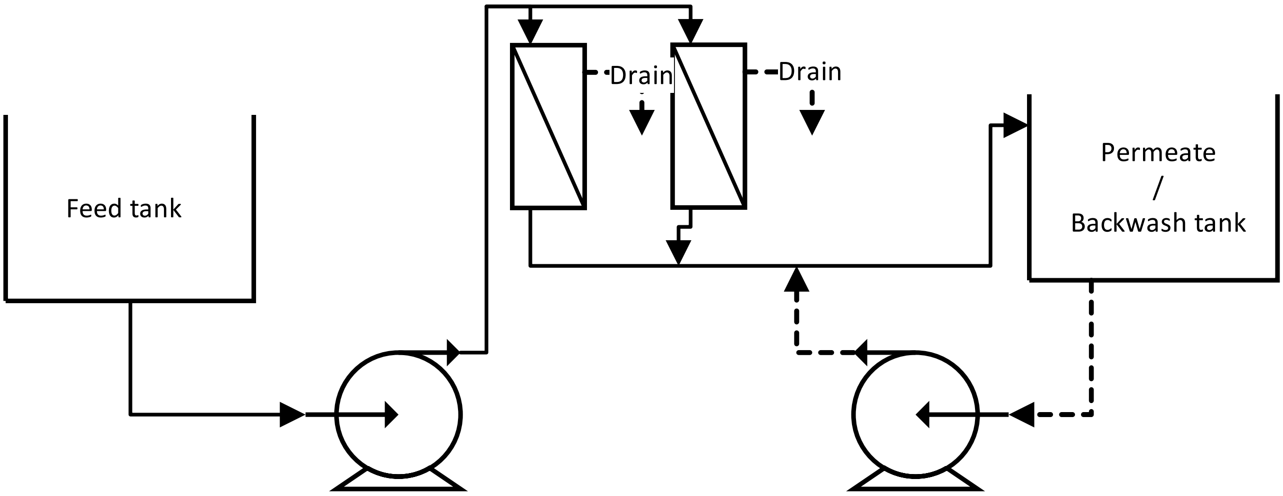

Figure 4 Simplified schematics of the UF skid

The UF in the IMPROVED containers is based on two identical hollow fiber modules from INGE model Dizzer P 4040-6.0 operated in parallel. The nominal membrane pore size is 20 nm. One of the modules can be isolated from the system by closing down manual valves in case the required permeate flowrate can be achieved with one module at higher flux. The system automatically alternates between filtration, drain, backwash and forward flush modes. In filtration the permeate tank is filled first before outputting water to the next technology. During drain cycle the modules are drained of water and the filtered suspended solids. During backwash the water is rapidly pushed in the opposite direction and the filtered cake material is dislodged from the membrane surface. Finally, the feed space of the modules is flushed before going back into filtration mode. The permeate tank was not dosed with chemicals – no chemically enhanced backwash, only normal backwash was used.

5. Results and Discussion

Ultrafiltration (UF)

The UF was operated throughout the whole testing period from 10th July until 7th of October 2024 - Figure 5:

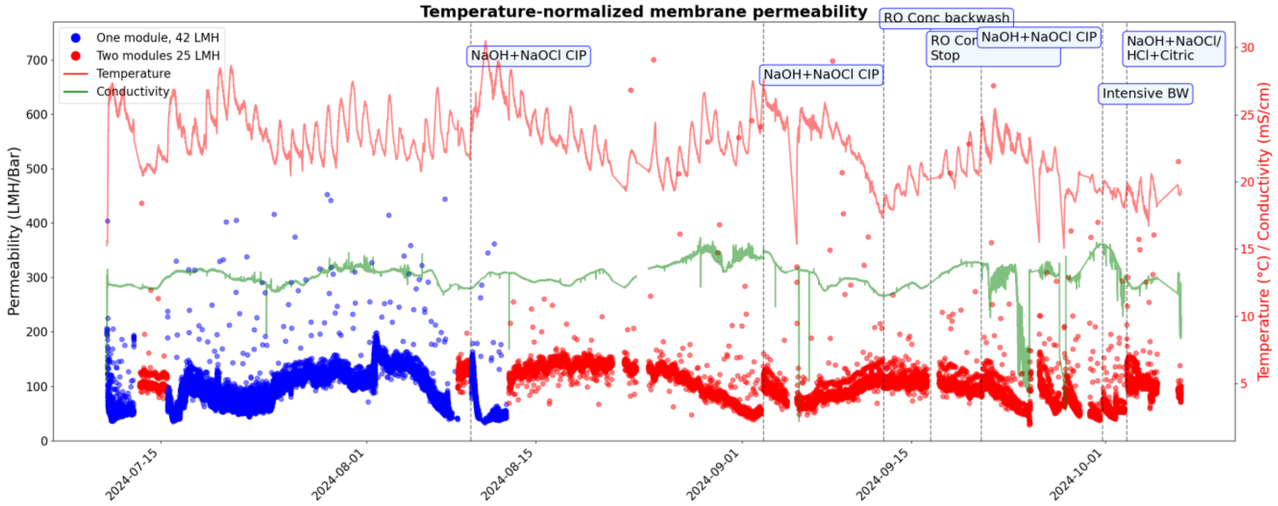

Figure 5 Temperature, Conductivity and normalized permeability of the UF in the testing period

The temperature normalized permeability of the UF is an indicator of the membrane fouling – a higher permeability means that the water needs less pressure to achieve the same water flux through the membrane. The ultrafiltration can be operated with one or two modules in parallel. When one module is operated, the flux needs to be higher in order to produce enough water for the RO step, therefore as a general guideline one module was operated at 42 Lmh, while 2 modules were operated at 25 Lmh. Initially the system was started with 1 module during the startup which was later switched to 2 module operation for a short period of time and then back to 1 module operation. The recovery of the UF was around 90%, however if this installation is to be built in real world, the UF concentrate would be returned to the settlers.

One very interesting period is the blue (single membrane) period before the first chemical cleaning. The membrane permeability initially started to decrease, followed by a gradual increase and a very sharp increase. Then the membrane performance started to decline, necessitating the need for chemical cleaning. Before the cleaning was done, the second membrane module was opened so that the UF could operate trouble free for the RO until cleaning was done (in red). It is noteworthy that the permeability with two membranes (one being supposedly fouled) was in this moment almost the highest in the testing period. This suggests that the fouling on the membrane is not permanent, and is in fact more of an issue of critical flux. Critical flux in ultrafiltration is the threshold flux value below which there is minimal or no irreversible fouling and a stable membrane performance can be maintained, while operating above this value leads to rapid and severe membrane fouling requiring frequent cleaning interventions. It represents the optimal operational point balancing productivity with sustainable long-term membrane performance. The process can be further augmented on full scale by also applying chemically enhanced backwashing (CEB) where chemicals are dosed in the backwashing tank. During the tests, the system was set to operate at 70% of the determined critical flux, but if CEB is also applied, possibly the system can be operated at up to 100% of the critical flux.

After the first chemical cleaning with NaOH and sodium hypochlorite, the system was placed in single module operation. The permeability was very high after the cleaning, suggesting that the cleaning was effective, but after a few hours, the permeability value reduced sharply once more. The system was since then placed into 2 module operation which improved the permeability immediately. This confirms the theory about the critical flux of the UF. The reversibility of the membrane permeability as a function of flux suggests that the fouling is not caused by biofouling, which is logical as most of the easily biodegradable components would be removed by the WWTP.

For a short period of time the backwashing of the UF was done with RO concentrate. There are several advantages of using such scheme – the higher osmotic pressure of the RO concentrate can shock any biology that grows on the UF (30-40 mS/cm RO concentrate vs 10-15 mS/cm feed water), the recovery of the UF can be increased since no permeate will be used in the backwashing, longer backwashing can be done possibly improving the effect and others. Unfortunately, no clear improvement was seen in the UF permeability and a lot of negative effects were seen at the RO, so the use of RO concentrate in the UF backwashing was quickly stopped.

It should be noted that decreasing the flux to 25 Lmh by opening the second module helped the performance of the system a lot, but it seemed that in some periods (e.g. around 1st Sep) the performance of the UF seemed to have worsened once more, suggesting that the water quality has a variable nature. Unfortunately, no turbidity was measured throughout the tests to support this observation. It should be noted that more than 50 production plants contribute to the influent of the WWTP and disturbances of any of them like shutdowns and startups can lead to challenges in the operation of the WWTP and hence the effluent quality can be variable in its nature. It is therefore imperative to do longer testing periods in order to have realistic tests.

Towards the end of September, the water quality seemed to have worsened once more. A cleaning in place with NaOH and sodium hypochlorite, followed by citric acid was done in order to see if iron-based fouling is causing issues with the UF, but this seemed to have no extra effect than the normal NaOH and sodium hypochlorite cleaning. Towards the end of September the permeability could be restored shortly with intensive backwashes (longer backwash cycles), but the effect lasted no more than a few hours. In a real-world installation, the system could benefit form an online turbidity sensor that is used for control of the duration of the backwash and filtration cycles as well as flux depending on the feed water quality.

The pressure of the UF can be seen in Figure 6:

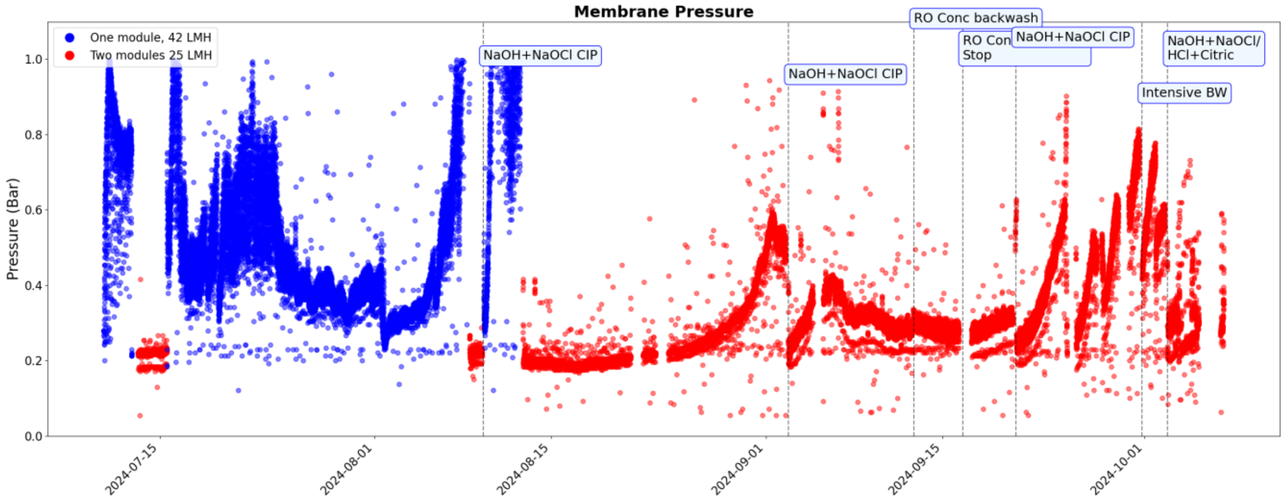

Figure 6 Pressure during the operation of the UF

The pressures were reaching values of 1 bar when operated with a single module and rarely exceeded 0.6 bar when operated in dual module mode. The pressure increases during the exploration period were inversely correlated with the decreases in normalized permeability (Figure 5), thereby also indicating fouling.

The exact flux values during the operation of the UF can be seen in Figure 7:

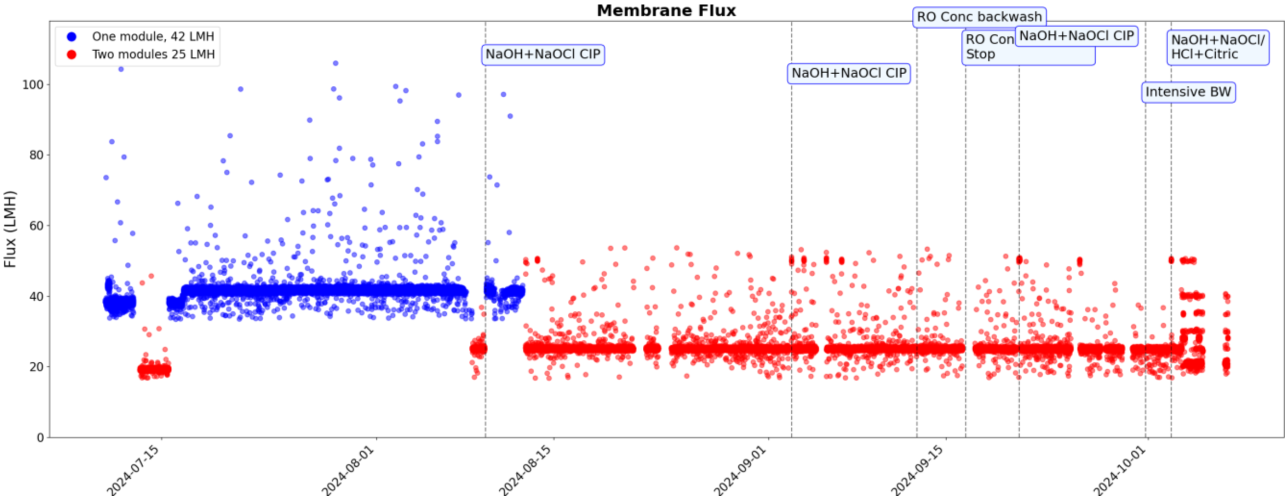

Figure 7 Flux settings of the ultrafiltraion

As a general rule of thumb one module was operated at 42 Lmh and two modules were operated at 25 Lmh, but the exact values were somewhat different in the first weeks of operation. Towards the last week of operation an algorithm was implemented that automatically would evaluate the critical flux of the UF and set the system flux lower than the critical flux value. This is the reason why the flux had several values after the NaOH and NaOCl followed by HCl and Citric acid cleaning.

At times in the feed of the pilots, plastic fill from columns of certain plants at the BASF site and large pieces of sludge from the WWTP were observed, affecting the influent water quality of the WWTP. Combined with the suspected variable water quality, a robust pretreatment is recommended if the system is to be built at BASF. Some options are coarse strainers or screens (1-5 mm) followed by self-cleaning fine screens (100-500 microns) to remove larger particles, debris, and suspended solids. Additional pre-treatment might include media filtration of sand/anthracite. Chemical pre-treatment with coagulation may also be considered, but this would increase the operational cost and carbon footprint of the UF.

Overall the UF process was rather stable and did not need many cleaning in place events.

Feed water quality

In order to give a good comparison of the feed water quality during the RO and the CCRO tests, the mean, median and other statistical values are given Table 1. It should be noted that these were done during two separate periods and therefore the feed water quality was different.

Table 1 Feed water quality for the RO and CCRO experimental periods

Parameter	Period	Mean	Median	Standard Deviation	Minimum	Maximum	Sample Size
Chloride, ppm	RO	2979.46	2919.00	224.26	2672.80	3389.00	14
Chloride, ppm	CCRO	3481.20	3429.75	379.07	2546.50	4377.00	24
Fluoride, ppm	RO	9.29	9.17	0.82	8.10	11.25	14
Fluoride, ppm	CCRO	9.11	8.80	2.03	5.39	15.55	24
Phosphate, ppm	RO	8.64	10.00	2.72	0.00	10.00	14
Phosphate, ppm	CCRO	4.94	4.60	4.45	0.10	20.23	24
Conductivity, µS/cm	RO	11765.00	11905.00	690.17	10810.00	13210.00	14
Conductivity, µS/cm	CCRO	12496.25	12310.00	897.03	11020.00	14480.00	24
Nitrate, ppm	RO	8.72	2.31	13.25	0.10	47.74	14
Nitrate, ppm	CCRO	8.10	2.67	13.25	0.10	61.75	24
Nitrite, ppm	RO	0.32	0.10	0.48	0.10	1.69	14
Nitrite, ppm	CCRO	4.23	0.10	11.97	0.10	43.60	24
Sulfate, ppm	RO	1136.63	1138.50	183.81	918.00	1610.00	14
Sulfate, ppm	CCRO	1059.54	1035.60	157.43	730.98	1433.50	24
TOC, ppm	RO	26.97	27.86	9.41	2.73	42.02	14
TOC, ppm	CCRO	27.15	28.41	7.75	13.80	40.77	24
Aluminum, ppm	RO	0.09	0.09	0.01	0.06	0.12	14
Aluminum, ppm	CCRO	0.07	0.07	0.02	0.04	0.11	24
Barium, ppm	RO	0.03	0.03	0.01	0.02	0.04	14
Barium, ppm	CCRO	0.02	0.02	0.00	0.02	0.03	24
Calcium, ppm	RO	55.43	55.08	3.09	49.50	60.18	14
Calcium, ppm	CCRO	62.52	61.29	5.46	53.82	75.00	24
Iron, ppm	RO	0.11	0.12	0.04	0.03	0.15	14
Iron, ppm	CCRO	0.07	0.07	0.03	0.01	0.14	24
Potassium, ppm	RO	53.81	53.17	3.82	47.30	62.63	14
Potassium, ppm	CCRO	50.26	48.43	5.86	41.00	61.00	24
Magnesium, ppm	RO	89.17	87.35	10.80	76.17	108.13	14
Magnesium, ppm	CCRO	112.36	112.25	7.64	96.76	130.00	24
Manganese, ppm	RO	0.03	0.03	0.01	0.02	0.05	14
Manganese, ppm	CCRO	0.03	0.03	0.01	0.01	0.05	24
Sodium, ppm	RO	2890.48	2921.50	177.82	2612.61	3190.41	14
Sodium, ppm	CCRO	3059.36	3078.50	217.65	2649.73	3596.00	24
Silica, ppm	RO	1.64	1.91	0.59	0.57	2.41	14
Silica, ppm	CCRO	2.17	2.07	0.58	1.20	4.00	24

Reverse osmosis (RO)

The system was operated in conventional reverse osmosis mode between July 10 and August 13. The RO was operated without a cartridge filter since it was placed after the ultrafiltration. The flux and the recovery were always kept at 17 Lmh and 66 %, respectively. The temperature and conductivity normalized membrane permeability for that period, which is an indication of the membrane fouling can be seen in Figure 8:

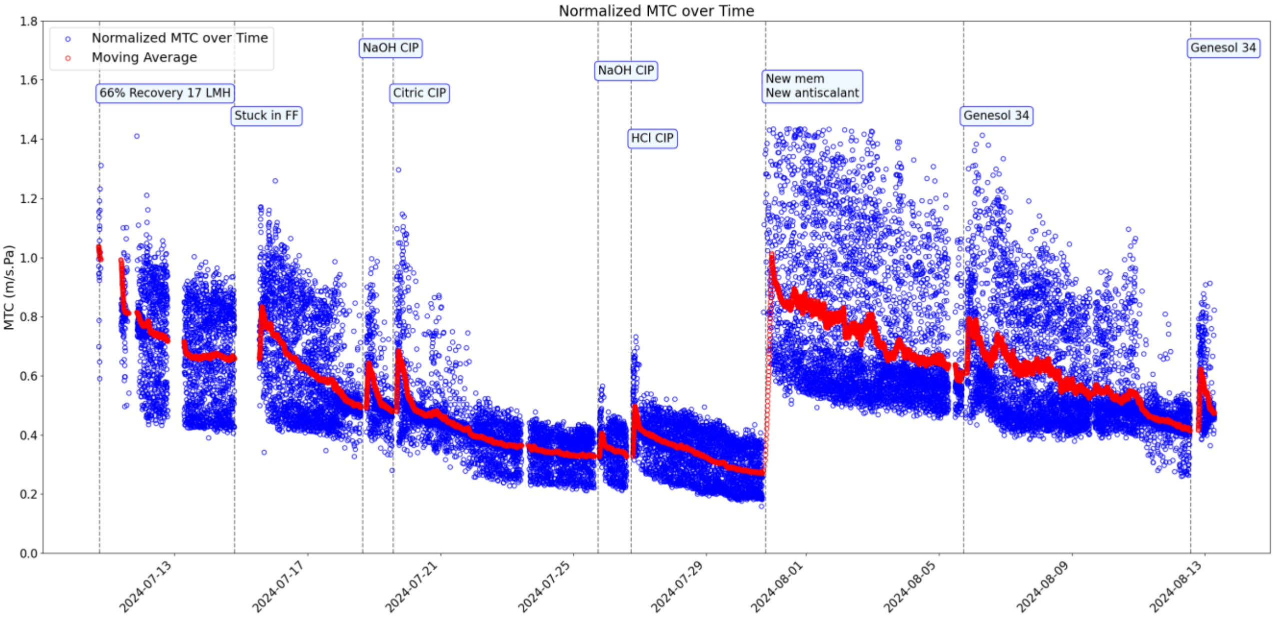

Figure 8 Normalized membrane mass transfer coefficient (MTC for the RO)

The system was operated with COSUN Carboxyline 25-30UP at 5ppm dosage until July 30th. The membrane MTC started to decrease rapidly in the first week of operation. An initial rapid decline is somewhat expected in the first days to a certain degree as the membrane will inevitably be fouled and the active layer of the membrane will become compressed. However, the magnitude of this decline is much larger than usual. July 14, the system became stuck in forward flush mode over the weekend. In this mode the feed water is just pumped through the feed channel, flushing it. Interestingly the membrane permeability was nicely restored after the system was placed back in operation.

To counteract the rapid decline of permeability a cleaning in place with NaOH at pH 12, followed the next day by citric acid and HCl cleaning at pH 2 was done, but the effect of those cleanings was very short (a few hours). The rapid decline of the membrane continued and another cleaning was done with NaOH, followed by HCl on the next day. This had a minor effect on the membrane permeability, but ultimately the membrane MTC continued to decline until eventually the pressure exceeded 40 bar (Figure 14) and the membrane was replaced. A sample of the membrane was taken and examined; results can be found in the membrane autopsy section. Overall, the results showed a visually clean membrane with no obvious signs of scaling or fouling.

On July 30th a new BW30 PRO-4040 membrane was placed and the antiscalant was replaced with Genesys LF again dosed at 5 ppm in the feed. The performance of the membrane experienced similar declining trend. Here a cleaning of Genesol 34 was attempted at 3 % dosage and pH 12. The Genesol 34 special RO cleaner contains Iminodisuccinic acid (a chelating agent) and non-ionic surfactant. Given that the cleaner is used at high pH it offers a wide cleaning action for organic fouling, inorganic fouling, iron removal via chelation and removal of hydrophobic foulants via the surfactant. However, this cleaner also did not have a lasting or significant effect. Towards the end of the experiment another cleaning was done, but it was again unsuccessful.

There was no significant feed channel pressure drop increase throughout the tests, indicating no particulate fouling or biological fouling inside the feed spacer (Figure 9). The lack of feed channel pressure drop increase also confirms that no cartridge filter was needed for the RO, although the system recirculates over 90 % of the concentrate to the feed tank so there is a risk that biological formation or scale can potentially form in the feed tank, blocking the membrane.

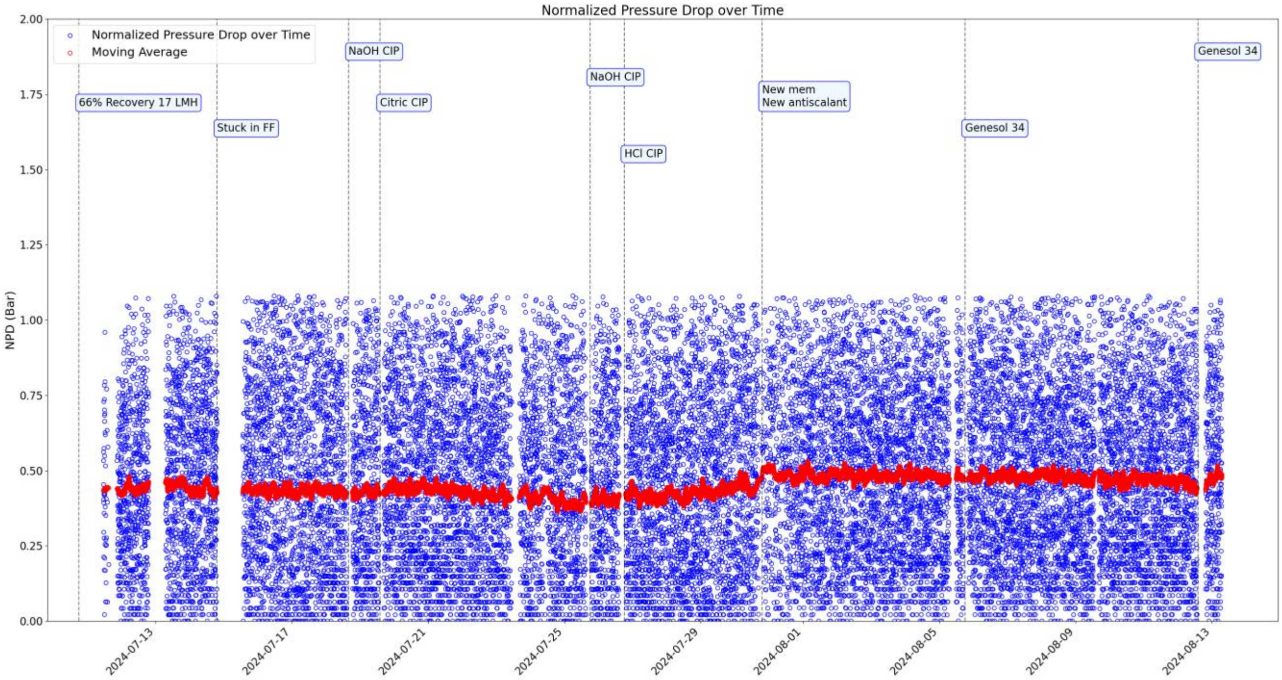

Figure 9 Feed channel pressure drop during the RO tests

The permeate conductivity in RO mode varied between 250 and 500 µS/cm - Figure 10

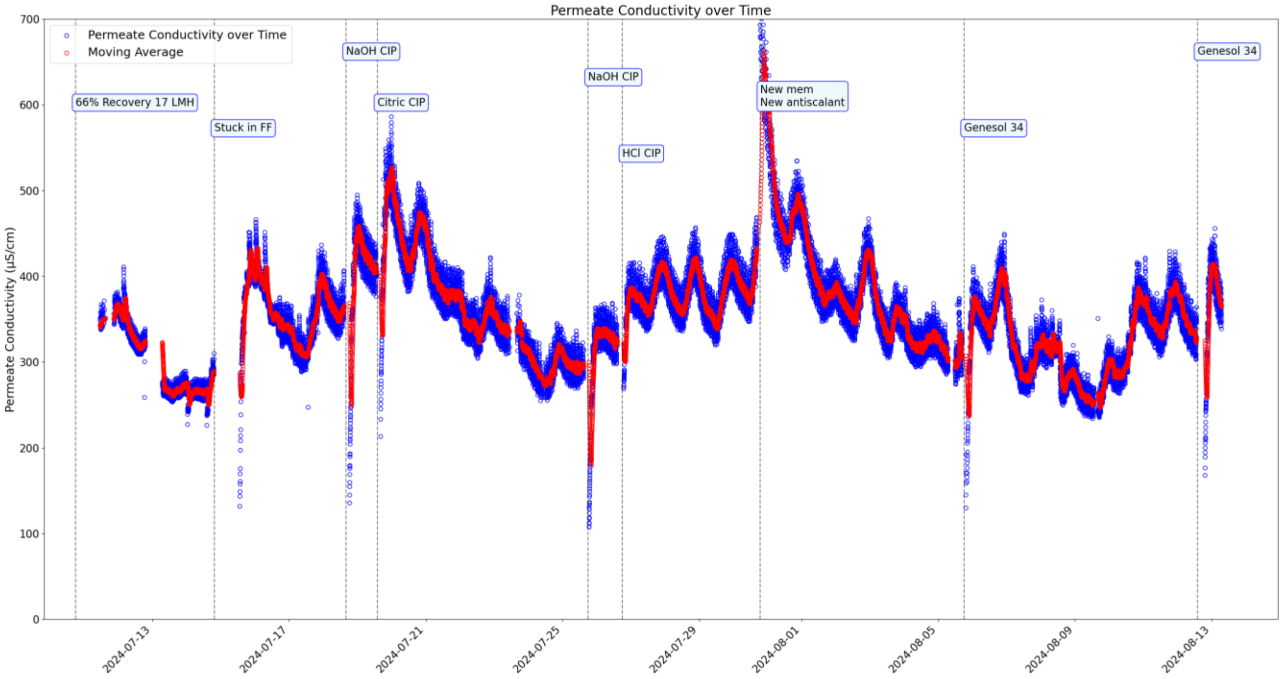

Figure 10 Permeate conductivity in RO mode

The normalized salt passage was rather stable at around 0.7-0.8 %, which is normal for this membrane. Increased normalized salt passage may speak of membrane damage but this is not observed here - Figure 11.

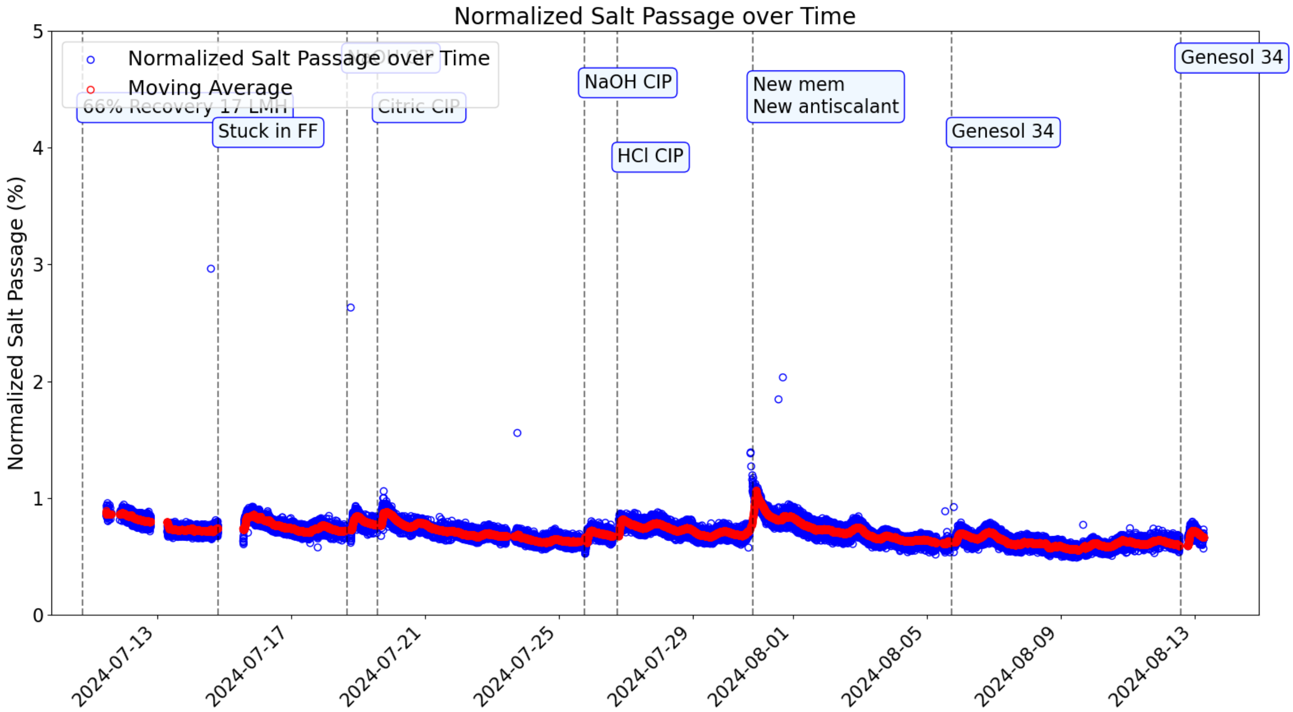

Figure 11 Normalized salt passage in RO mode

Overall, the performance of the conventional RO on this stream was very troublesome and the membranes experienced serious fouling after only 2 weeks of operation. The suspected fouling that is accumulating on the membrane is expected to be of organic nature with low biodegradability to pass the WWTP of BASF, smaller than 20 nm to pass the UF and resistant to acids and bases in the 2-12 pH range. The temporary minor effect of recovery of the membrane permeability after the system was stuck in forward flush mode suggests that the fouling is slowly soluble in water.

Why is RO normalization necessary

The normalized MTC is a representation of the membrane permeability (flux over applied pressure), where the temperature effects are taken into account and the pressure is the hydraulic pressure corrected for the osmotic pressure of the water. In this way a clear trend of the membrane fouling evolution can be observed much faster compared to just looking at the raw pressure value. In reverse osmosis the temperature improves the permeability by ~3 % with each degree, meaning that even small temperature variations have a huge effect on the membrane permeability. Similarly, the effluent of the WWTP has a high conductivity (Figure 13) and the osmotic pressure of the feed water varies between 14 and 18 bar (Figure 14). This can lead to very large daily swings in the pressure, making the true trends of the membrane fouling (Figure 15).

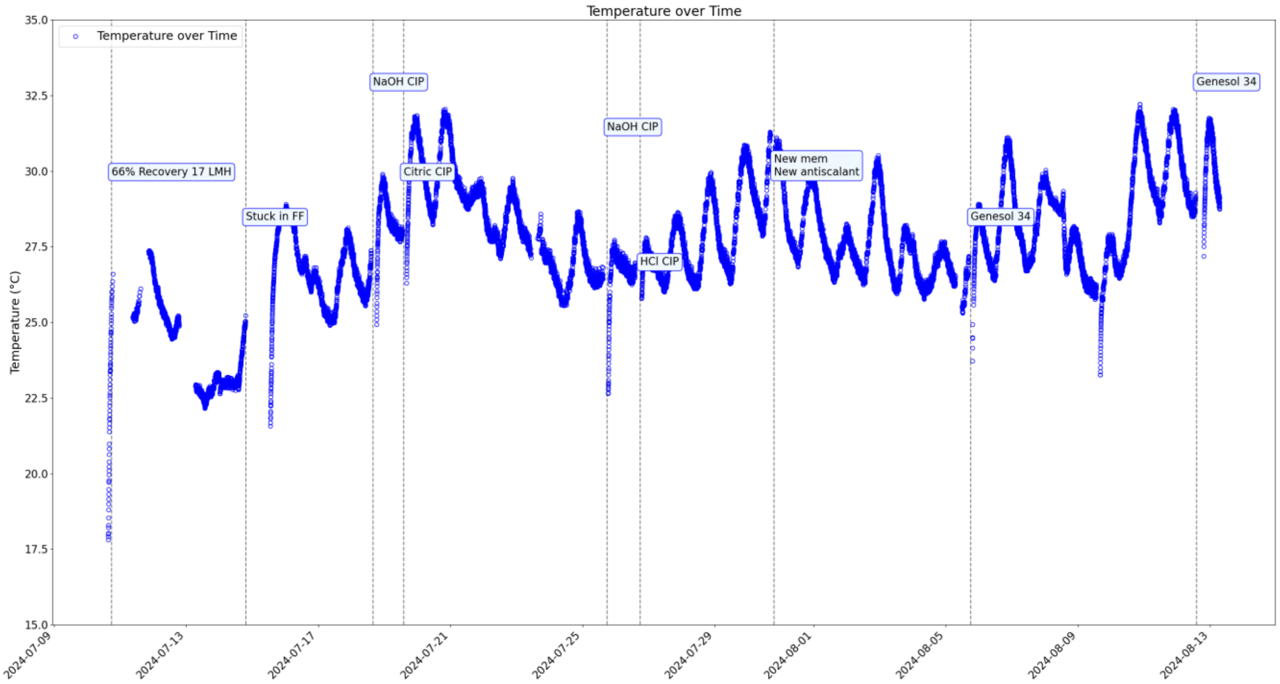

Figure 12 Temperature variations during the RO period

The conductivity of feed as well as feed and concentrate conductivity of the membrane can be seen in Figure 13. It should be noted that the feed conductivity is the raw conductivity of the incoming WWTP effluent. The reason why the membrane feed conductivity is much higher stems from the recirculating nature of the RO. Since a single element recovery is typically around 15%, in order to reach higher recoveries and still have sufficient flowrate in the feed channel of the RO membrane, a recirculation is done. This simulates the conditions in the last elements of the last stage of a conventional reverse osmosis installation, that are typically the most challenging due to the higher concentration of scaling elements and foulants.

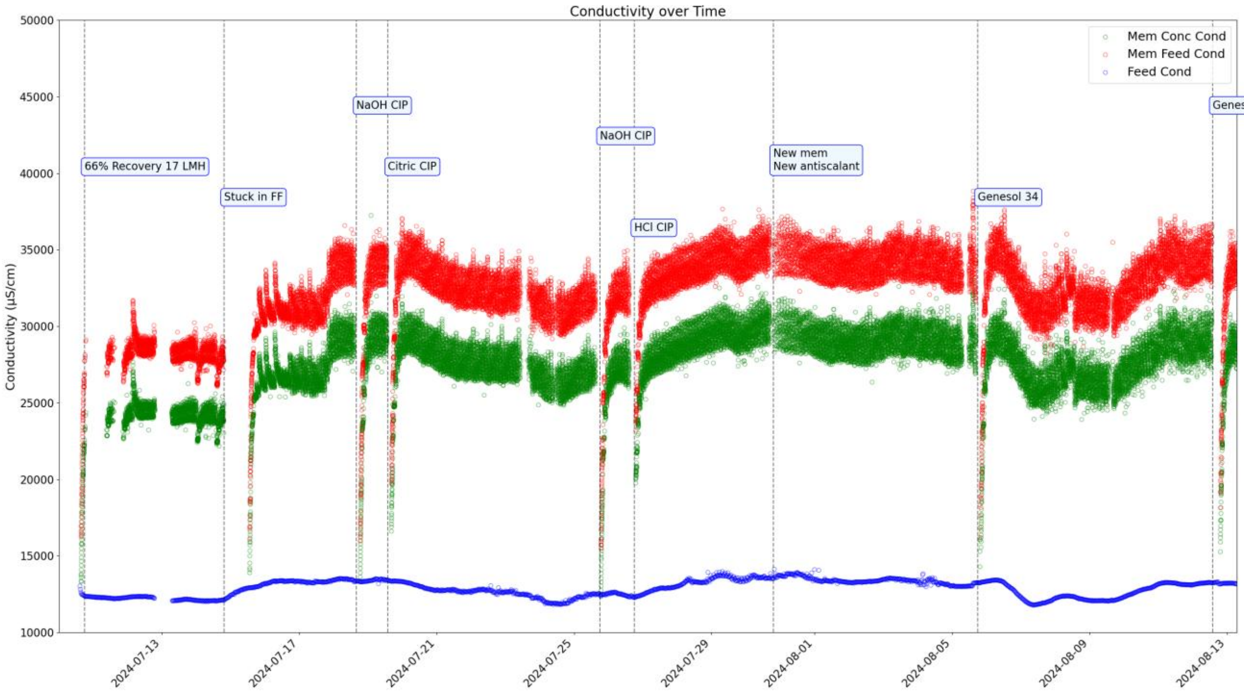

Figure 13 Conductivity on the feed and concentrate sides of the RO membrane as well as the feed conductivity.

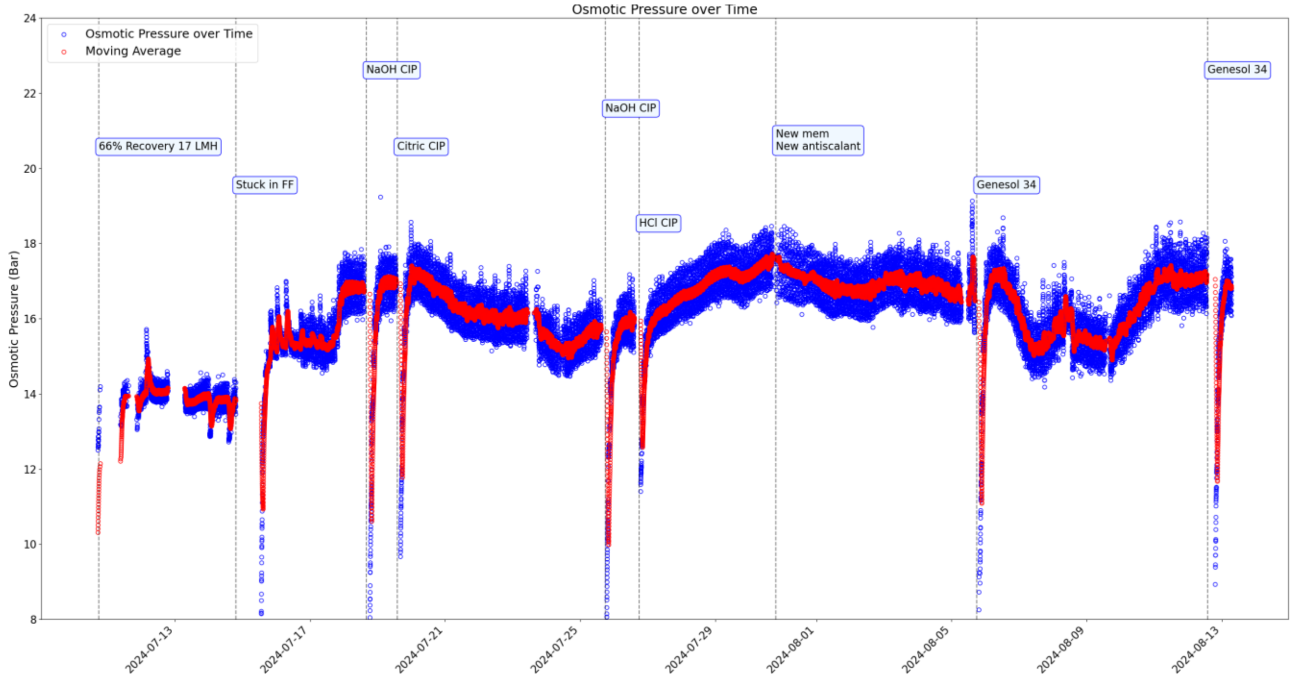

Figure 14 Average osmotic pressure of the feed and concentrate in the RO

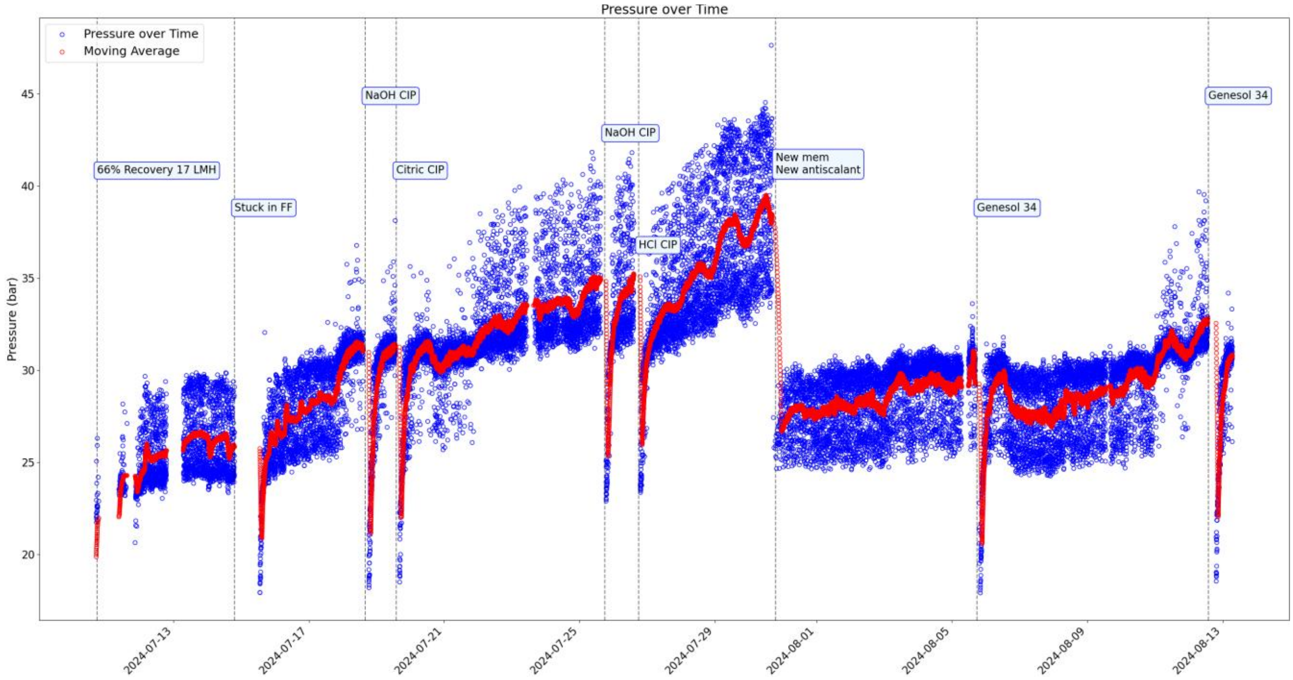

Figure 15 Average feed side pressure of the reverse osmosis

One thing that is not taken into consideration by the RO normalization is the concentration polarization. The concentration polarization happens as the ions are rejected on the membrane surface creating a localized concentration gradient. The ions need to migrate back into the bulk of the channel and ultimately the concentration on the membrane is always somewhat higher than the bulk. To facilitate the migration of ions back into the bulk of the channels, a certain fluid velocity is needed inside the channels. Typically, the DuPont Wave RO system design program recommends a minimum concentrate flowrate of 1.66 m^3/h, while the pump of the pilot can only achieve 1 m^3/h. Therefore, the concentration polarization is somewhat more pronounced in the pilot. Initially when the membrane MTC was plotted a very low value was obtained Figure 16:

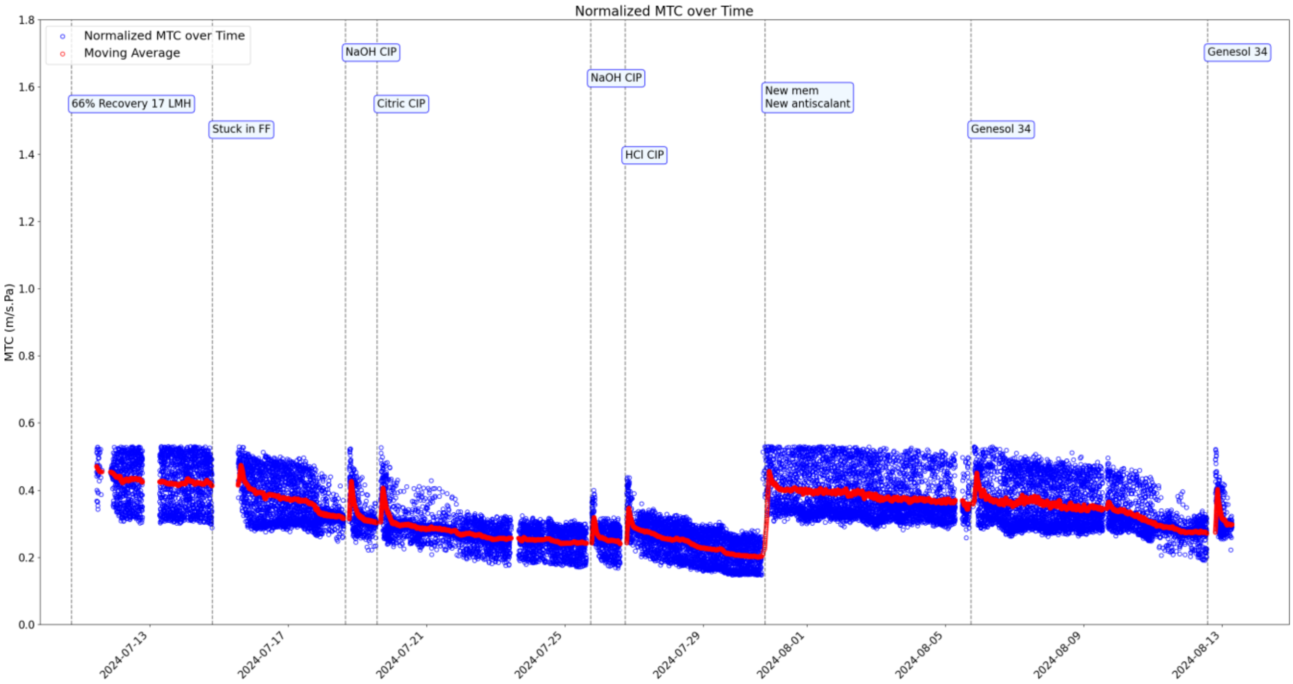

Figure 16 Membrane MTC for the RO membrane without the concentration polarization taken into account

The influence of concentration polarization is often neglected in RO normalization, however when the osmotic pressure is in the order of 15 bar as it is in this case, a 30 % concentration polarization would mean 5 bar extra pressure is needed for the water to achieve the same flux solely due to concentration polarization. Typically, a new BW30PRO 4040 membrane has a permeability of around 1.3 m/s.Pa. Therefore, in order to achieve meaningful values for the MTC in Figure 8 the osmotic pressure in the feed and concentrate side of the membrane was multiplied by a factor of 1.3, assuming 30 % concentration polarization.

Closed Circuit Reverse osmosis (CCRO)

The CCRO was started on 13th of August and was operated until the 7th of October. The Genesys LF antiscalant was used with 5ppm dosage in the feed (7th of October until 22nd of September) and no cartridge filter was used. Here it is important to underline again that the CCRO used in the study was not an official system offered by DuPont. UGent was given an explicit permission to modify its skid into CCRO by DuPont within the AquaSPICE trials, but the system can have subtle changes that may not perform in the same way as an official CCRO system.

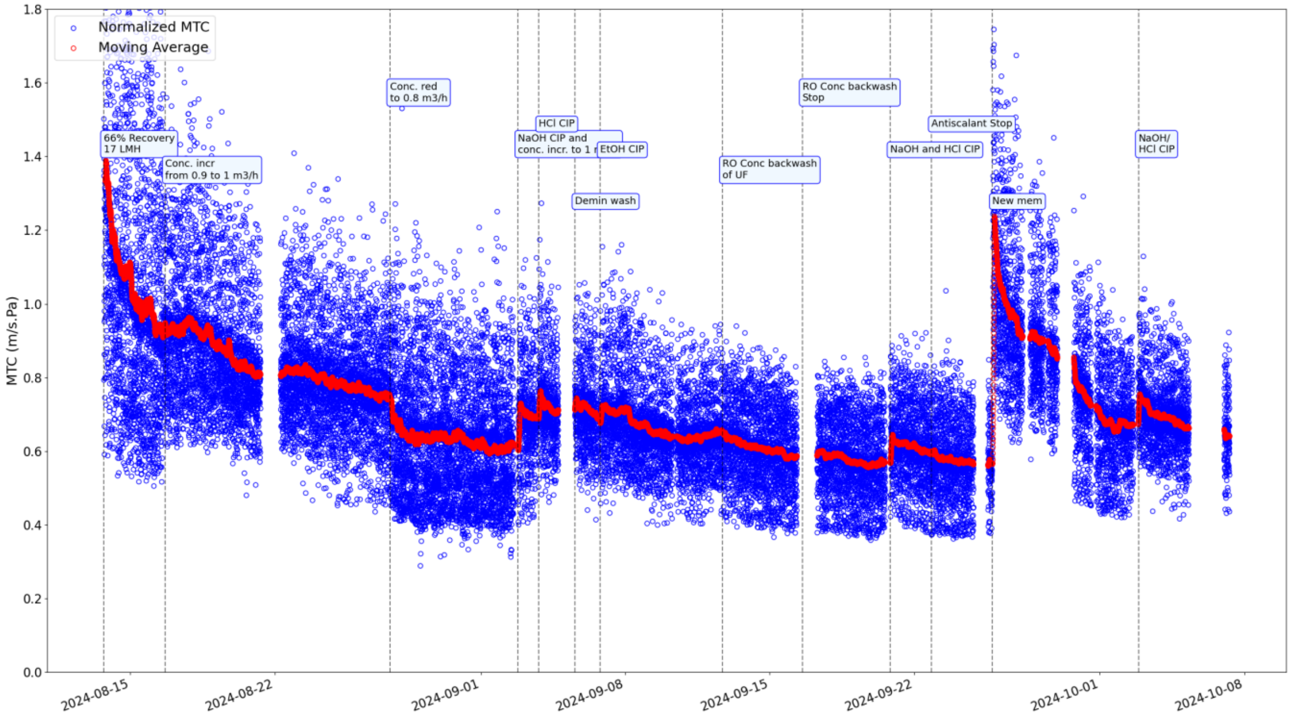

Figure 17 Membrane MTC of the CCRO

The experiments were performed again at 66% recovery and 17 Lmh flux (Figure 17). After 3 days of operation it was noticed that in CCRO mode the concentrate flowrate was even lower than the RO at 0.9 m^3/h due to different programming. To resolve this the pump flowrate was increased to 1m^3/h concentrate flowrate. In order to test the influence of concentrate flowrate of the system, the concentrate was then decreased to 0.8 m^3/h in the period 27/08 until 2/09. While the MTC expectedly decreased in value (due to the higher concentration polarization), the rate of MTC decline was not significantly different. After the system was placed back in 1 m^3/h concentrate flowrate, a cleaning in place with NaOH at pH 12 was simultaneously performed, followed by HCl cleaning at pH 2 on the next day. Similarly to the RO, these cleanings in place had no lasting effect on the membrane MTC. After this two more experimental CIPs were done with ethanol (10-15%) as well as a demin wash. The reasoning was that the ethanol might desorb the hypothetical foulant from the membrane surface and the demin wash was done to try to redissolve the fouling. None of these treatments worked successfully.

From Sep 12 until Sep 16 the UF was backwashed with RO concentrate. This, however, posed a serious problem for the UF and, as a result, also affected the CCRO, leading to a sharp increase in the conductivity of the CCRO permeate (Figure 18). Moreover, it seemed to also have a negative influence on the MTC as well. One possible explanation for this negative effect on the MTC and membrane conductivity is that biofouling and/or scaling may be forming inside the UF backwash tank. When the UF is backwashed these will be filtered on the permeate side of the UF and will eventually end up in the CCRO feed once the UF is placed back in filtration.

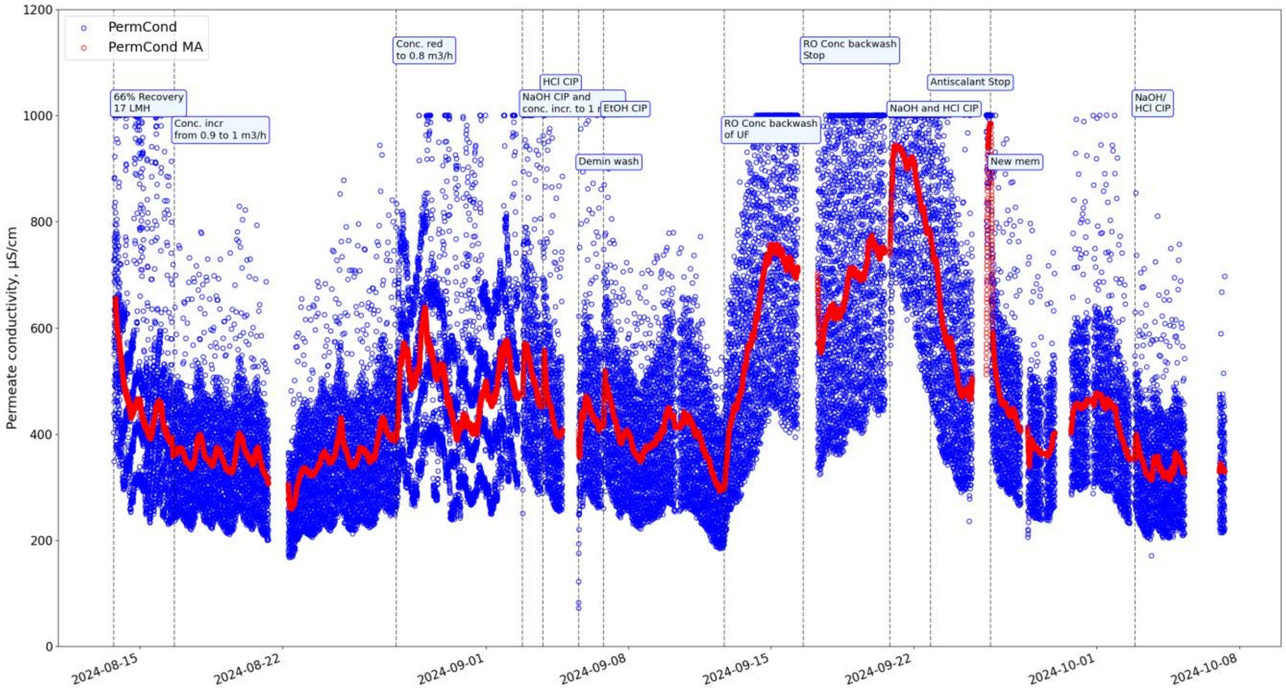

Figure 18 Permeate conductivity in CCRO mode

The CCRO permeate conductivity was around 400 µS/cm when the concentrate flowrate was 1 m^3/h, which is similar to the conductivity in RO mode. Once the backwash with RO concentrate was started at the UF, the RO permeate increased tremendously in value, even reaching the maximum value of the sensor at 1000 µS/cm, therefore the moving average value is not accurate in this region.

At this point suspicions that the membrane was damaged arose. The membrane was cleaned in place with NaOH, immediately followed by HCl cleaning which initially increased the conductivity of the permeate, but later caused it to return to values of around 450 µS/cm. Unfortunately, due to operator error the membrane was over pressurized to over 60 bar (25th September), which caused it to become damaged (large conductivity spike just before the "New mem" marker) and it was replaced on Sep 25th. The new membrane had similar values to the old values of 400 µS/cm before the over pressurization, proving that the previous membrane was not damaged before the over pressurization and that the bad quality was due to the UF backwashing with RO concentrate.

It is best not to compare the raw conductivity as it depends on the temperature and feed conductivity. Instead, it is better to compare the normalized salt passage (Figure 19). The values of normalized salt passage are about 10-20 % higher than the RO (Figure 11), which could be due to incomplete flushing of the CCRO during the brine flush cycle leading to higher conductivity on the feed side of the membrane. Also, in CCRO mode immediately after the flushing the conductivity is very high because of the lower flux values in this mode.

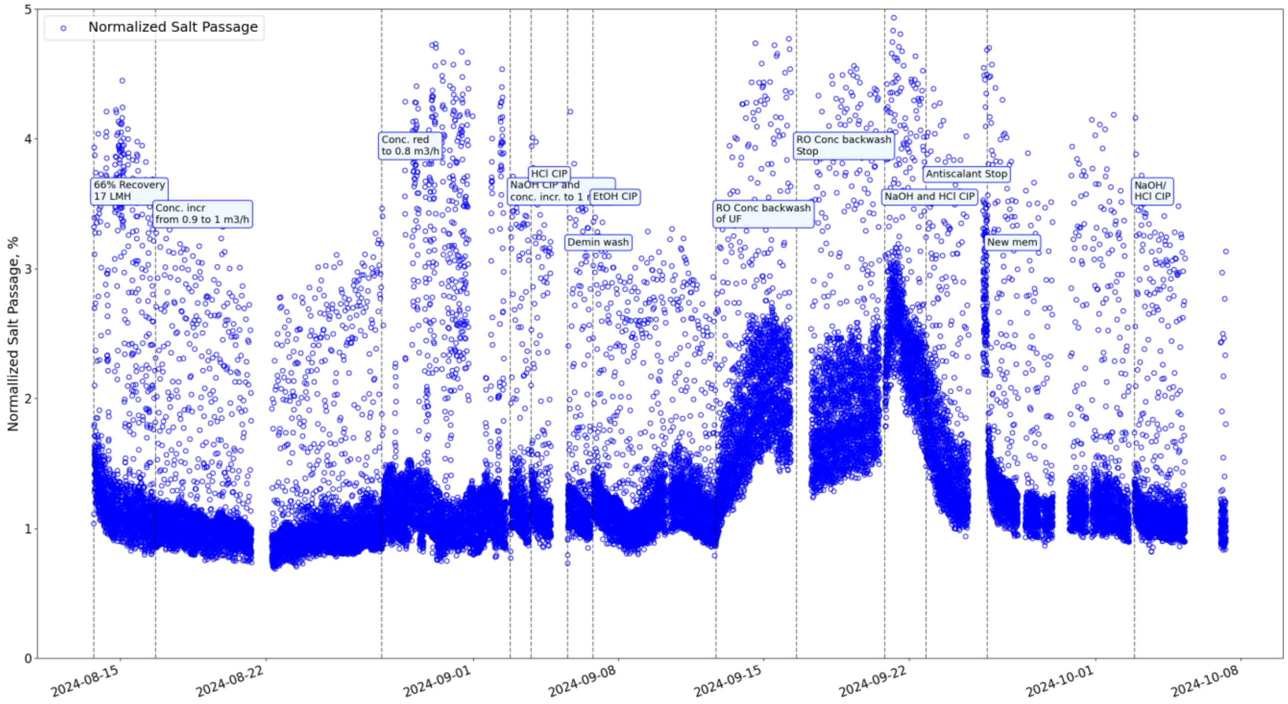

Figure 19 Normalized salt passage in CCRO mode

Laboratory analysis of the water produced with RO and CCRO

The produced water was sampled 3x per week and was then analyzed in the lab of BASF - Table 2. Please note:

Table 2 Quality of the treated water using RO and CCRO. To make a better comparison of the quality produced by the two technologies, both are given one below the other. But the reader is warned that the feed quality may have been different in the two periods of operation (RO and CCRO). Also in the beginning of the tests, some measurement limits were higher during the RO period. To make a fair comparison, the reader is encouraged to look at the figures in Appendix 2.

Parameter	Period	Mean	Median	Standard Deviation	Min	Max	# Samples
Chloride, ppm	*RO*	*80.692*	*78.100*	*14.794*	*58.800*	*117.000*	*13*
Chloride, ppm	CCRO	128.396	111.6	55.250	81.100	346.000	24
Fluoride, ppm	*RO*	*0.100*	*0.100*	*0.000*	*0.100*	*0.100*	*13*
Fluoride, ppm	CCRO	0.170	0.100	0.175	0.100	0.950	24
Phosphate, ppm	*RO*	*6.154*	*10.000*	*4.865*	*0.000*	*10.000*	*13*
Phosphate, ppm	CCRO	0.114	0.100	0.080	0.000	0.440	24
Conductivity, µS/cm	*RO*	*287.231*	*274.0*	*46.161*	*218.000*	*397.000*	*13*
Conductivity, µS/cm	CCRO	471.083	399.0	224.456	276.000	1376.000	24
Nitrate, ppm	*RO*	*1.014*	*0.1*	*1.585*	*0.100*	*5.220*	*13*
Nitrate, ppm	CCRO	1.253	0.465	1.765	0.100	8.010	24
Nitrite, ppm	*RO*	*0.118*	*0.100*	*0.061*	*0.100*	*0.330*	*13*
Nitrite, ppm	CCRO	0.182	0.100	0.182	0.100	0.760	24
Sulfate, ppm	*RO*	*0.866*	*0.850*	*0.351*	*0.290*	*1.740*	*13*
Sulfate, ppm	CCRO	9.716	3.020	16.152	0.510	79.000	24
TOC, ppm	*RO*	*1.557*	*2.000*	*0.705*	*0.295*	*2.000*	*14*
TOC, ppm	CCRO	0.626	0.582	0.387	0.249	2.310	24
Aluminum, ppm	*RO*	*0.017*	*0.010*	*0.023*	*0.010*	*0.098*	*13*

Aluminum, ppm	CCRO	0.010	0.010	0.000	0.010	0.012	24
Barium, ppm	*RO*	*0.010*	*0.010*	*0.000*	*0.010*	*0.010*	*13*
Barium, ppm	CCRO	0.010	0.010	0.000	0.010	0.010	24
Calcium, ppm	*RO*	*0.046*	*0.033*	*0.033*	*0.010*	*0.149*	*13*
Calcium, ppm	CCRO	0.559	0.177	0.919	0.040	4.300	24
Iron, ppm	*RO*	*0.010*	*0.010*	*0.000*	*0.010*	*0.010*	*13*
Iron, ppm	CCRO	0.010	0.010	0.000	0.010	0.010	24
Potassium, ppm	*RO*	*1.425*	*1.381*	*0.387*	*0.881*	*2.500*	*13*
Potassium, ppm	CCRO	2.114	1.815	0.732	1.500	4.700	24
Magnesium, ppm	*RO*	*0.047*	*0.045*	*0.015*	*0.028*	*0.080*	*13*
Magnesium, ppm	CCRO	0.994	0.261	1.706	0.072	8.000	24
Manganese, ppm	*RO*	*0.010*	*0.010*	*0.000*	*0.010*	*0.010*	*13*
Manganese, ppm	CCRO	0.010	0.010	0.000	0.010	0.010	24
Sodium, ppm	*RO*	*58.405*	*58.440*	*9.836*	*46.465*	*86.000*	*13*
Sodium, ppm	CCRO	97.288	83.763	48.603	58.000	297.000	24
Silica, ppm	*RO*	*0.012*	*0.010*	*0.005*	*0.010*	*0.030*	*13*
Silica, ppm	CCRO	0.115	0.010	0.394	0.010	2.000	24
Strontium, ppm	*RO*	*0.010*	*0.010*	*0.000*	*0.010*	*0.010*	*13*
Strontium, ppm	CCRO	0.013	0.010	0.008	0.010	0.048	24

A figure of the time series for each component is given in Appendix 2. While a table summary is a more compact way to represent the data, often it gives a simplified picture of the real situation. Therefore, the reader is encouraged to browse through the time series figures in the Appendix. Some things to note are that the TOC is much larger in the RO period, due to an unnecessary dilution in a few of the initial samples, leading to high low detection limit of 2ppm. This was later addressed and the later detection limit for TOC was 0.2ppm. Similar things can be seen for the phosphate.

Another noteworthy detail is that the quality of the CCRO in the table view is significantly worse compared to the RO. This can be explained by the worsened quality of the CCRO when the UF was backwashed with CCRO concentrate (see previous section for details) and the one sample with the membrane which was damaged by very high pressures. A better way to compare the two technologies is to plot the rejection - Figure 20 and Figure 21.

The elements with higher average rejections are displayed in Figure 20 and the elements with lower average rejection are displayed in Figure 21. In case the feed or the RO permeate measured value is below detection limit, the rejection is depicted with a triangular marker. From this comparison it can be seen that while the CCRO has marginally lower product quality, the two technologies produce very similar water.

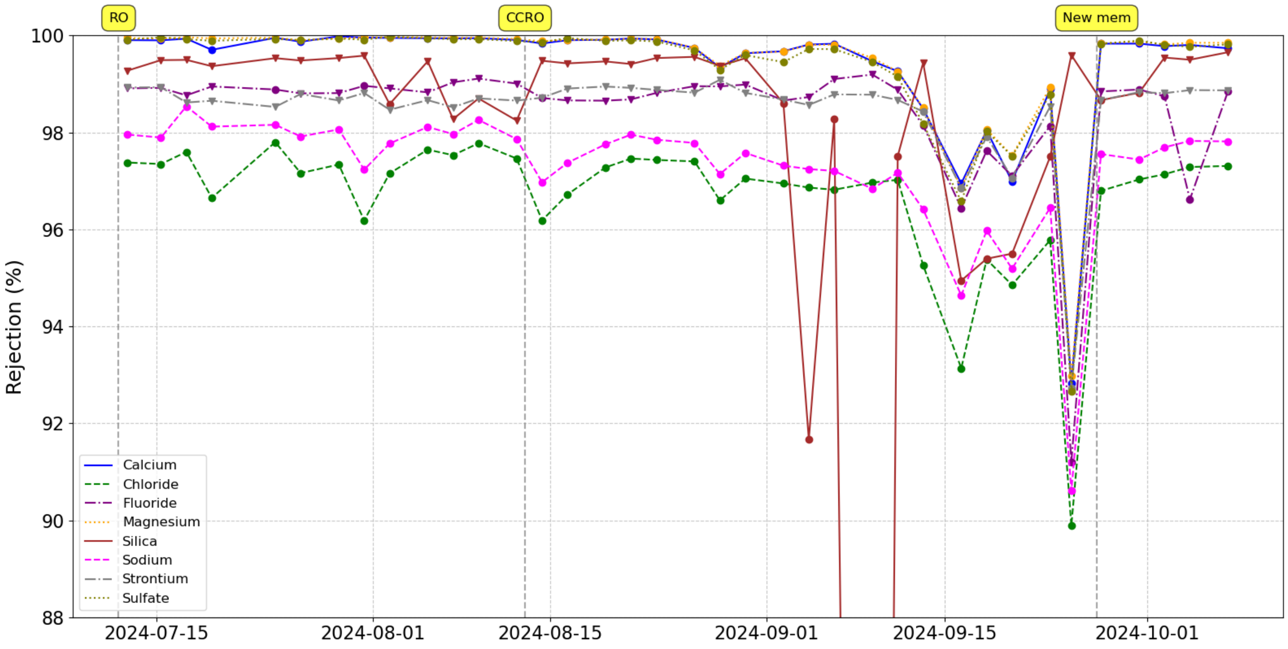

Note: Triangular markers (▼) indicate values where Feed or RO-P was below detection limit

Figure 20 Rejection of the RO based on the feed values. High rejection component group

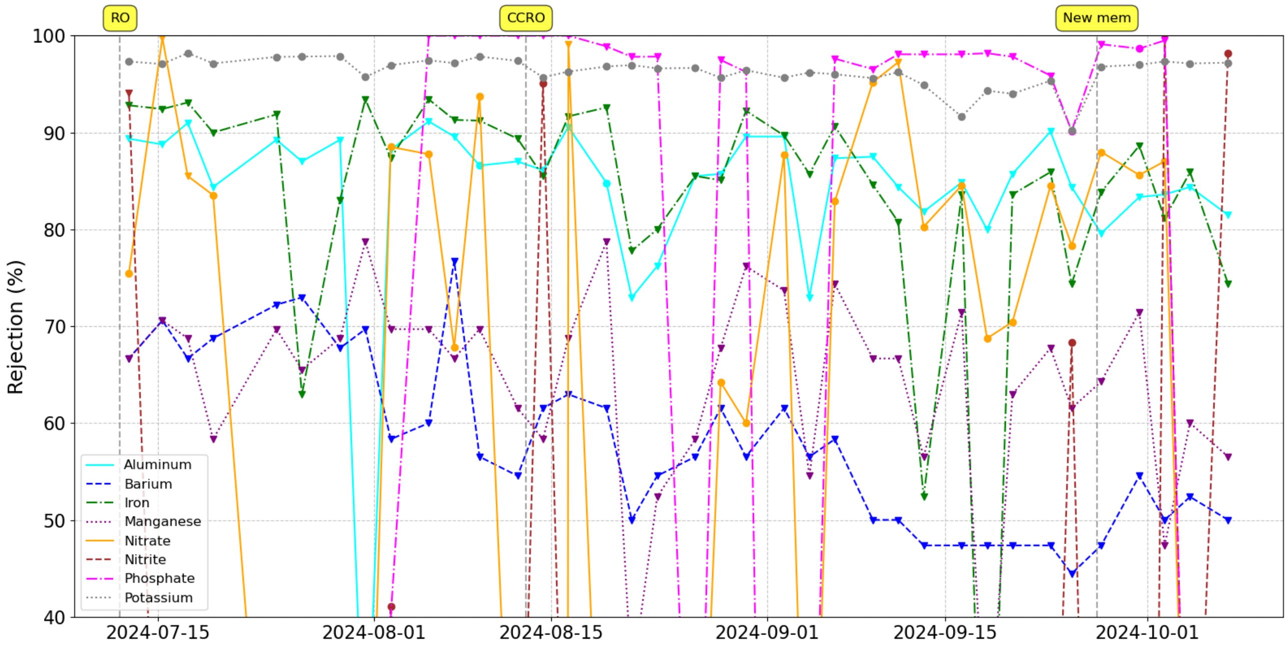

Note: Triangular markers (▼) indicate values where Feed or RO-P was below detection limit

Figure 21 Rejection of the RO based on the feed values. Low rejection component group

The TOC and conductivity rejection during the trials is listed below in Figure 22

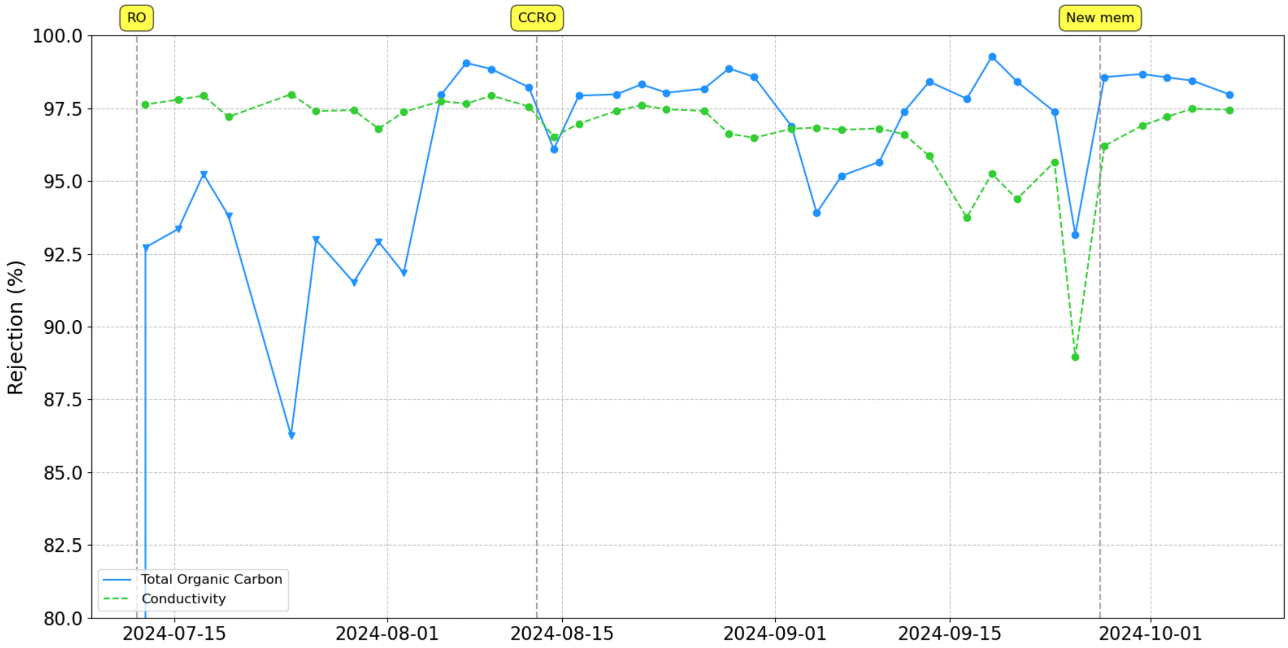

Note: Triangular markers (▼) indicate values where Feed or RO-P was below detection limit

Figure 22 Rejection of conductivity and TOC during the trials for RO and CCRO

It is interesting to note that the TOC rejection for CCRO is in fact higher than it is for RO but the first 2 weeks of operation were done with a high limit of detection (hence the triangular markers). Also, the TOC composition cannot be guaranteed to be the same in the two testing periods of RO and CCRO which can also affect the rejection.

6. Membrane autopsy

Membrane autopsy of the membrane operated in RO mode on 01/08

Figure 23 Membrane autopsy on 01/08. Operation in RO mode

Overall, this membrane looks to be in pristine state, which is surprising given the severe reduction in permeability and the increased operational pressure. The thin fouling layer was very easy to rub off with a finger revealing a shiny polymer layer. While organic fouling can indeed lower the MTC, we would expect a much thicker fouling layer based on the MTC reduction during the trials. In terms of scaling the expected scalants before and after an addition of Genesys LS antiscalant can be seen in Figure 24:

RECOMMENDED ANTISCALANT Genesys LF

Select Product

	$CaCO_3$	$CaSO_4$	$BaSO_4$	$SrSO_4$	CaF_2	$Ca_3(PO_4)_2$	Fe	SiO_2	Al	Mn	$Mg(OH)_2$
%Conc. Untreated	138.16	13.33	739.58	11.40	3837.01	0.00	51.99	9.94	19.89	37.13	0.06
%Conc. Treated	40.89	4.76	14.79	1.14	10.96	0.00	3.47	6.63	12.92	2.48	0.00

Recovery (%) 66.0

Feed Water pH 7.5

Temperature (°C) 30.0

DOSAGES

For Scale Control - Feed	2.96	mg/L
For Iron Control - Feed	0.10	mg/L
Total Feed Dose	3.06	mg/L
Dose In Conc.	9.00	mg/L
Operating Time	24.00	Hr/day
Set Dosing Pump To	186.08	mL/hr
Daily Requirement	6.03	kg/day
Acid not required	0.00	mg/L
Acid Requirement	0.00	kg/day

Figure 24 Scaling prediction from the Membrane Master 5 software

The main scalants expected in the simulation are $CaCO_3$, $BaSO_4$, CaF_2 and Fe. They should all be nicely controlled by the antiscalant, however in our experience some elements such as Fe can scale on the membrane regardless of the scaling prediction or precipitate with organics. In order to further investigate an ICP-OES analysis was done on a membrane after microwave digestion. In order to differentiate between acid-soluble Ca in $CaCO_3$ and the acid insoluble CaF_2 and $CaSO_4$, a second ICP-OES analysis was done after soaking the membrane first for over 1h in 1M HCl acid. The results can be seen in **Error! Reference source not found.** and **Error! Reference source not found.**

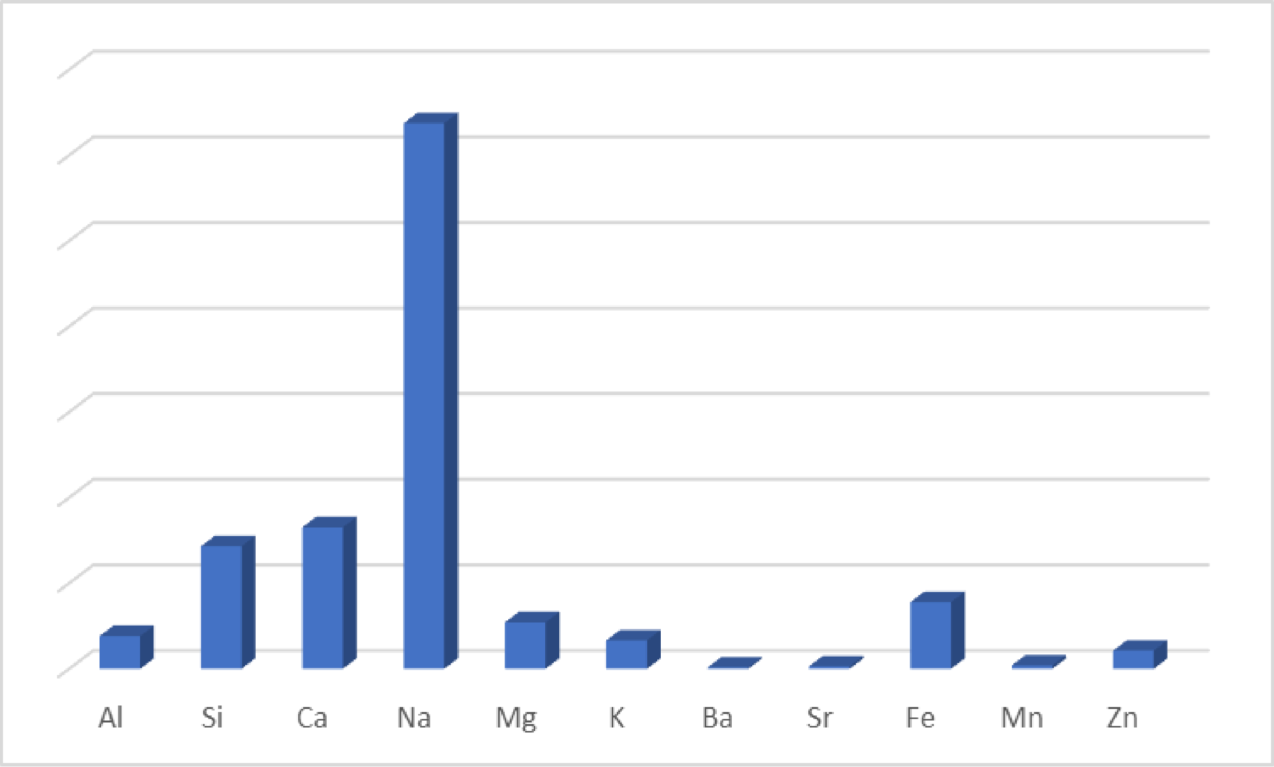

Figure 25 Relative concentrations in the ICP-OES analysis after microwave digestion. Numbers are not given as they are meaningless in a relative concentration context.

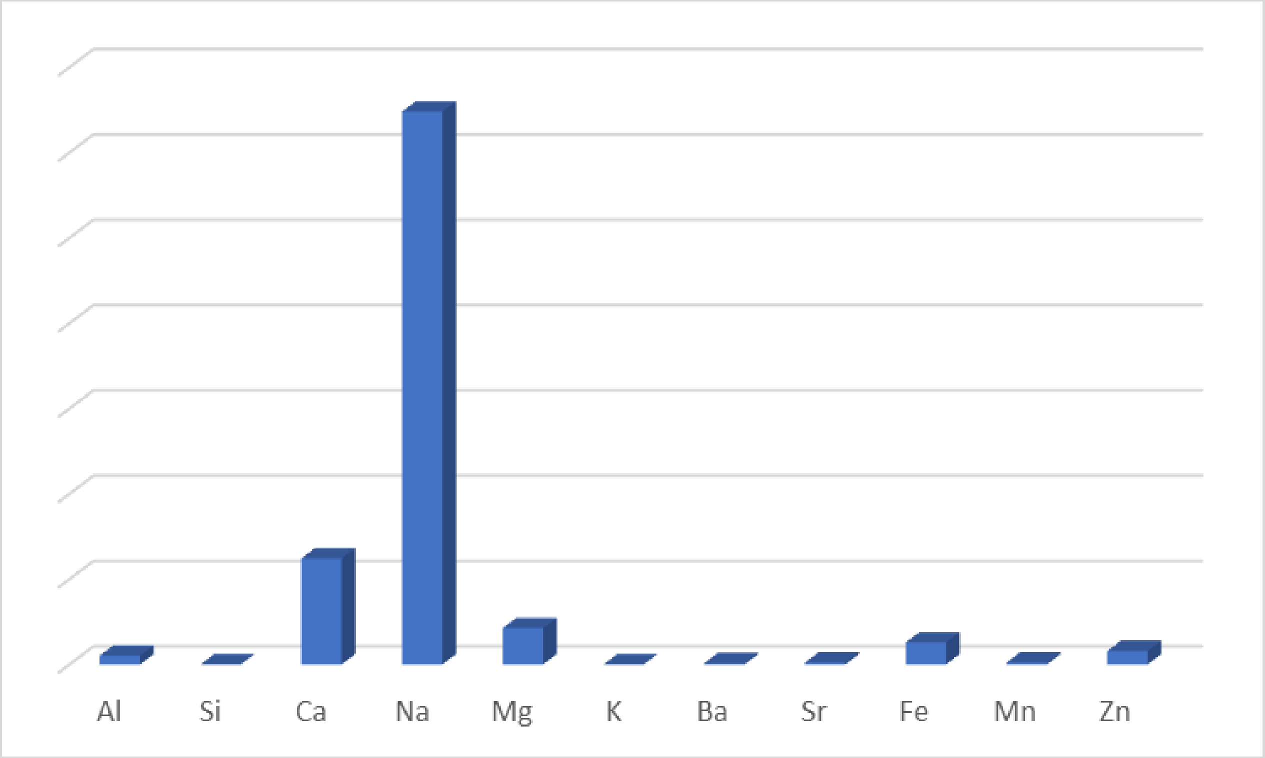

Figure 26 Relative concentrations in the ICP-OES analysis after soaking the membrane for over 1h in HCl followed by microwave digestion. Numbers are not given as they are meaningless in a relative concentration context.

It should be noted that Na is not a scaling element, so this is in fact background contamination. In the membrane that was only digested we see Si, Ca, Mg and Fe scaling, while in the HCl soaked membrane we see only Ca, Mg and Fe. Based on this we can conclude that the Si in **Error! Reference source not found.** is colloidal silica that ended up on the membrane, since Si cannot be dissolved in HCl. Mg is also surprising to see as it is not predicted as a scaling risk in the Membrane Master 5 software. Moreover, in both analyses the Na is the predominant element, even though it’s just a background element and therefore there are no signs of significant scaling.

Optical microscopy was also performed on some of the fouling found on the membrane. Overall, no visible scaling can be observed Figure 27.

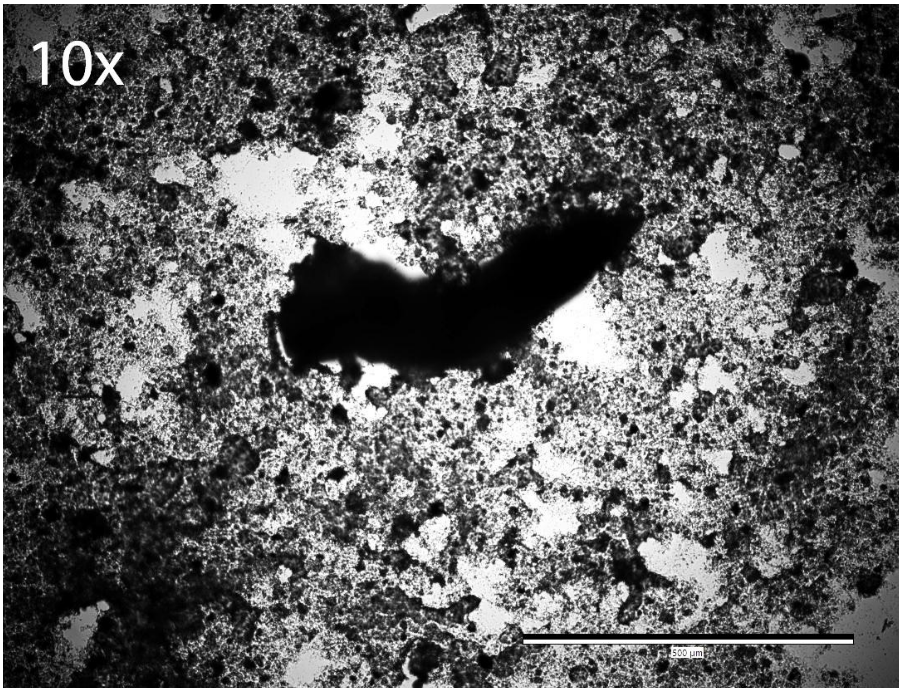

Figure 27 Optical microscopy of the fouling scraped from the membrane

Suspicions that large-molecule organic fouling may be settling on the membrane surface due to chemical affinity with the membrane material arouse. Components that are under suspicion are: Polyvinyl alcohol (PVA), Carboxymethyl cellulose (CMC), Polyethylene glycols (PEG), Polyacrylates (in superabsorbing polymers or flocculation etc).

A battery of tests were performed on several membranes and can be summarized in table Table 3:

Table 3 Tests performed on membrane autopsies and their outcomes

Date membrane harvested	Test type	Conclusion
16/08	BASF GC-MS (Gas Chromatography-Mass Spectrometry)	No specific organic components found on the membrane
16/08	BASF FTIR (Fourier Transform Infrared Spectroscopy)	Biological nature of the fouling
16/08	BASF XRF scan (X-ray Fluorescence Spectroscopy)	Fe, Ca, Cl, S, P, Zn elements detected on the membrane
01/10	UGent LC-MS (Liquid Chromatography-Mass Spectrometry)	No specific organic components found on the membrane
01/10	UGent HPLC-MS High-Performance Liquid Chromatography-Tandem MS)	No specific organic components found on the membrane
01/10	UGent py-GC-MS (Pyrolysis-Gas Chromatography-Mass Spectrometry)	No specific organic components found on the membrane
01/10	UGent SEM-EDS (Scanning Electron Microscopy with Energy Dispersive X-ray Spectroscopy)	Some silica fouling as well as a sulfur containing nodes

Since no specific components were found on the membrane, it was concluded that the fouling was likely of natural organic matter and some minor scaling. However, the possibility still exists that the fouling is from a specific foulant for example the superabsorbent polymers, but was not able to be identified with the testing methods.

Permeability tests using the fouled membrane at the UGent laboratory

Some of the membranes harvested during the autopsy were tested in the lab in terms of permeability. The original idea of this was to test if ethanol could be used to extract a potential foulant of organic nature. The summary of the tests can be found in Table 4:

Table 4 Permeability tests in the lab using membranes harvested from the autopsies

Harvested	Conditions	Storage	Coupon	LMH/bar	Salt rejection, %
16-Aug	20 bar, 1g/l NaCl	In NaHSO3 in fridge	Fouled	3.3	98.8
16-Aug	20 bar, 1g/l NaCl	In NaHSO3 in fridge	Washed	3.4	98.5
16-Aug	20 bar, 1g/l NaCl	In NaHSO3 in fridge	15% Ethanol	3.5	98.9
16-Aug	20 bar, 1g/l NaCl	In NaHSO3 in fridge	30% Ethanol	4.0	99.1
16-Aug	20 bar, 1g/l NaCl	Dry in packaging	New membrane	3.8	98.4
1-Oct	20 bar, 1g/l NaCl	Dry in fridge	Fouled	3.3	98.9

Analysis of the membrane permeability tests revealed interesting discrepancies between pilot and laboratory conditions. Membranes harvested on August 16 were preserved in sodium bisulfite solution and refrigerated, while the October 1st membrane sample was stored in a refrigerated plastic bag. Remarkably, laboratory testing showed these fouled membranes retained 80 % of their original permeability - exhibiting 3.3 LMH/bar compared to 3.8 LMH/bar for new membranes.

Simple mechanical cleaning by gentle rubbing with deionized water produced a modest improvement in permeability to 3.4 LMH/bar. More notably, in-situ ethanol cleaning trials, conducted by circulating 15 % and 30 % ethanol solutions through the membrane setup, showed promising results. The 30 % ethanol treatment not only enhanced permeability but also improved salt rejection performance, suggesting potential for this cleaning methodology in future applications.

The stark contrast between laboratory and pilot-scale performance warranted investigation. The leading hypothesis suggests that while the fouling layer may not significantly impact clean water permeability, it creates a stagnant boundary layer that intensifies concentration polarization effects. This theory is supported by two key operational differences:

1. Flow dynamics: The pilot system operated at approximately 10 cm/s cross-flow velocity, while laboratory tests maintained 20 cm/s (value to be verified), reducing concentration polarization effects in the latter.
2. Salinity conditions: Pilot tests processed feed water at 30-35 mS/cm conductivity, whereas laboratory tests used significantly lower salinity (1 g/L NaCl, equivalent to 2 mS/cm). The higher salinity in pilot operations would amplify concentration polarization effects at the membrane surface.
3.

These findings suggest that the fouling layer's impact on membrane performance is primarily through enhanced concentration polarization rather than direct permeability reduction, particularly under high-salinity conditions.

It was hypothesized that the fouling on the membrane had minor influence on the lab-scale compared to the pilot scale because the pilot scale was done at much higher conductivity of 30-35 mS/cm. New permeability tests were done at 34.5 mS/cm, but the permeability was again 20.7% lower compared to the nearly 50 % reduction in permeability on pilot scale. Ultimately it was concluded that this light fouling may help other fouling stick to the membrane and form a gel layer which is removed better in CCRO mode due to its flushing cycles. However, this hypothesis cannot be confirmed.

7. Conclusions

The three-month trial at BASF's wastewater treatment plant demonstrated both the potential and challenges of treating WWTP effluent for reuse as process water or a source for boiler feed water production.

1. Water Quality Achievement: Both RO and CCRO technologies successfully produced water meeting process water quality requirements (conductivity 300-800 µS/cm), with TOC levels below 1 ppm - potentially suitable a a source for boiler feed water production, exceeding the current source water quality (2-4 ppm TOC).
2. Ultrafiltration Performance: The UF system demonstrated stable operation when operated at an appropriate flux of 25 LMH with two modules, compared to unstable operation at 42 LMH with a single module. This indicates the existence of a critical flux threshold, below which membrane fouling is acceptable. The fouling was largely reversible with NaOH and NaOCl cleaning. Overall the water was challenging for the UF.
3. Conventional RO Limitations: The conventional RO system faced significant operational challenges, with severe membrane fouling occurring within 20 days of operation. The fouling proved irreversible despite multiple cleaning attempts using various chemical treatments (acids, bases, chelating agents, and non-ionic surfactants).
4. CCRO Advantages: The inhouse implemented mimic CCRO system showed superior fouling resistance compared to conventional RO, maintaining stable operation for five weeks with fouling tendencies reaching a plateau. Both systems operated at 17 LMH flux and 66% recovery, but CCRO demonstrated better long-term operational stability.
5. Membrane Fouling Characterization: Extensive membrane autopsy and analysis revealed that the fouling was primarily composed of natural organic matter with minor scaling components. Laboratory permeability tests suggested that concentration polarization effects due to a thin fouling layer, rather than a thick irreversible fouling layer, may be the primary cause of performance decline in the pilot scale.

For full-scale implementation, several recommendations emerge:

- Implementation of robust pre-treatment, possibly including sand filters, coarse strainers (1-5 mm) and fine screens (100-500 microns) may help with the UF stability issues and allow for operation at higher flux
- Operation of UF below critical flux, but also with chemically enhanced backwash
- Preference for CCRO over conventional RO for long-term operational stability and longer membrane lifetime due to less chemical cleanings
- Installation of online turbidity monitoring for automated control of backwash cycles of the UF
- Consideration of mixed pre-treatment strategies for variable water quality management

These findings demonstrate the technical feasibility of treating WWTP effluent for reuse, while highlighting the importance of appropriate technology selection and operating parameters for sustainable long-term operation.

Acknowledgments

The authors would like to acknowledge the European Commission for funding the AquaSPICE project. The AquaSPICE project has received funding from the European Union’s Horizon 2020 research and innovation programme under grant agreement No 958396.

AquaSPICE

This work was partly supported by the TOCADISCO project, funded by EFRO (Europees Fonds voor Regionale Ontwikkeling).

EFRO
EUROPEES FONDS
VOOR REGIONALE
ONTWIKKELING

Europese Unie

Mede gefinancierd
in het kader van de
respons van de Unie op
de COVID-19-pandemie

References

[1] M. H. P. M. B. M. H. J. C. L. Han Gu, "Operational optimization of closed-circuit reverse osmosis (CCRO) pilot to recover concentrate at an advanced water purification facility for potable reuse," *Desalination,* vol. 518, no. 115300, 2021.

[2] Dupont Water Solutions, "DesaliTec™ CCRO High Efficiency Smart Reverse Osmosis Systems," Dupont, [Online]. Available: https://www.dupont.com/brands/desalitec-ccro-high-efficiency-ro.html. [Accessed 14 February 2023].

[3] J. Huang, "EVALUATING OF CLOSED-CIRCUIT REVERSE OSMOSIS (CCRO) OF MUNICIPAL WASTEWATER - PILOT STUDY," Presented to the Faculty of California State Polytechnic University , Pomona, 2022.

[4] Lenntech, "Closed Circuit Reverse Osmosis," Lenntech, [Online]. Available: https://www.lenntech.com/products/membrane/ccro.htm. [Accessed 10 March 2022].

[5] H2O Engineering, "Closed-Circuit Reverse Osmosis (CCRO)," [Online]. Available: https://www.h2oengineering.com/technologies/closed-circuit-reverse-osmosis-ccro/. [Accessed 15 February 2023].

List of abbreviations

BGAC	Biological granular activated carbon
CapEx	Capital Expenditure
CCRO	Closed-circuit reverse osmosis
CIP	Cleaning in place
COD	Chemical oxygen demand
DO	Dissolved oxygen
EDR	Electrodialysis reversal
EDI	Electrodeionization
GAC	Granular activated carbon
IC	Inorganic carbon, ion chromatography
IEX	Ion exchange
IMPROVED	Integrale Mobiele PROceswater Voorziening voor een Economische Delta
MABR	Membrane aerated bioreactor
MB	Mixed bed resin
MTC	Mass transfer coefficient
NDP	Net Driving Pressure
NPD	Normalized Pressure Drop
NSP	Normalized salt passage
OpEx	Operational Expenditure
PFRO	Pulse-flow reverse osmosis
RO	Reverse osmosis
RO-P	RO permeate
SAC	Strong Acid Cation
TC	Total Carbon
TOC	Total organic carbon

8. Appendices

Appendix 1. Equations used in the RO normalization

$$SP = EC_p \times T_{cf\_EC} \times Q_{cf}$$

$$EC_p = 100 \times \frac{EC_{permeate}}{(EC_{feed} \times \left(log \frac{1}{1 - Recovery}\right))/Recovery}$$

$$T_{cf} = exp^{(U_{par} \times \left(\left(\frac{1}{T_{feed}+273.15}\right) - \left(\frac{1}{T_{ref}+273.15}\right)\right))}$$

Where U_{par} is the Dow membrane U-value, equal to 3200, EC_p is the recovery corrected permeate conductivity, T_{ref} is the reference temperature equal to 25 °C and T_{cf} is the conductivity corrected temperature.

$$NPD = dP \times Q_{cf} \times T_{cf}$$

$$dP = P_{feed} - P_{concentrate}$$

$$Q_{cf} = \left(\frac{Q_{vc}}{\frac{Q_{permeate} + Q_{concentrate}}{2}}\right)^m$$

$$Q_{vc} = \frac{Q_{feedn} + Q_{concentraten}}{2}$$

$$T_{cf} = \left(\frac{\eta_{ref}}{\eta_{feed}}\right)^n$$

Where NPD is normalized pressure drop [kPa], Q_{feedn} normalized design feed flow of the RO system [$m^3.h^{-1}$], $Q_{concentraten}$ normalized design concentrate flow [$m^3.h^{-1}$], T_{cf} is the viscosity corrected temperature, $Q_{vc}$is the viscosity corrected flow, η_{ref} and η_{feed} are reference and feed viscosity respectively, m and n are Dow membrane values, equal to 1.6 and 0.4, respectively.

$$MTC = \frac{Q_{permeate} \times T_{cf} \times 10^{-5}}{36 \times Q_{pemeate}}$$

$$NDP = ((\frac{P_{feed} + P_{concentrate}}{2} - P_{permeate}) \times 100) - (\frac{OP_{feed} + OP_{concentrate}}{2} - OP_{permeate})$$

$$T_{cf\_OP} = \frac{T_{feed} + 273.15}{T_{ref} + 273.15}$$

$$OP_{feed} = EC_{feed} \times EC_{OP\_feed} \times T_{cf\_OP}$$

$$OP_{concentrate} = EC_{concentrate} \times EC_{OP\_concentrate} \times T_{cf\_OP}$$

$$OP_{permeate} = EC_{permeate} \times EC_{permeate} \times T_{cf\_OP}$$

Where MTC is the mass transfer coefficient [m.S^{-1}.Pa^{-1}], NDP net driving pressure [kPa], OP osmotic pressure calculated for feed, permeate and concentrate [kPa] and T_{cf_OP} is the osmotic pressure corrected temperature.

Appendix 2. Laboratory analyses

The laboratory analysis was performed by BASF for conductivity, TOC, metals and anions. The samples were taken 3x per week on Monday, Wednesday and Friday. The results are plotted with the most important changes in the system operation listed as annotations on the top of the figures. It is important to notice that in case the value of a certain measurement is below detection limit, its marker is denoted with a triangular marker.

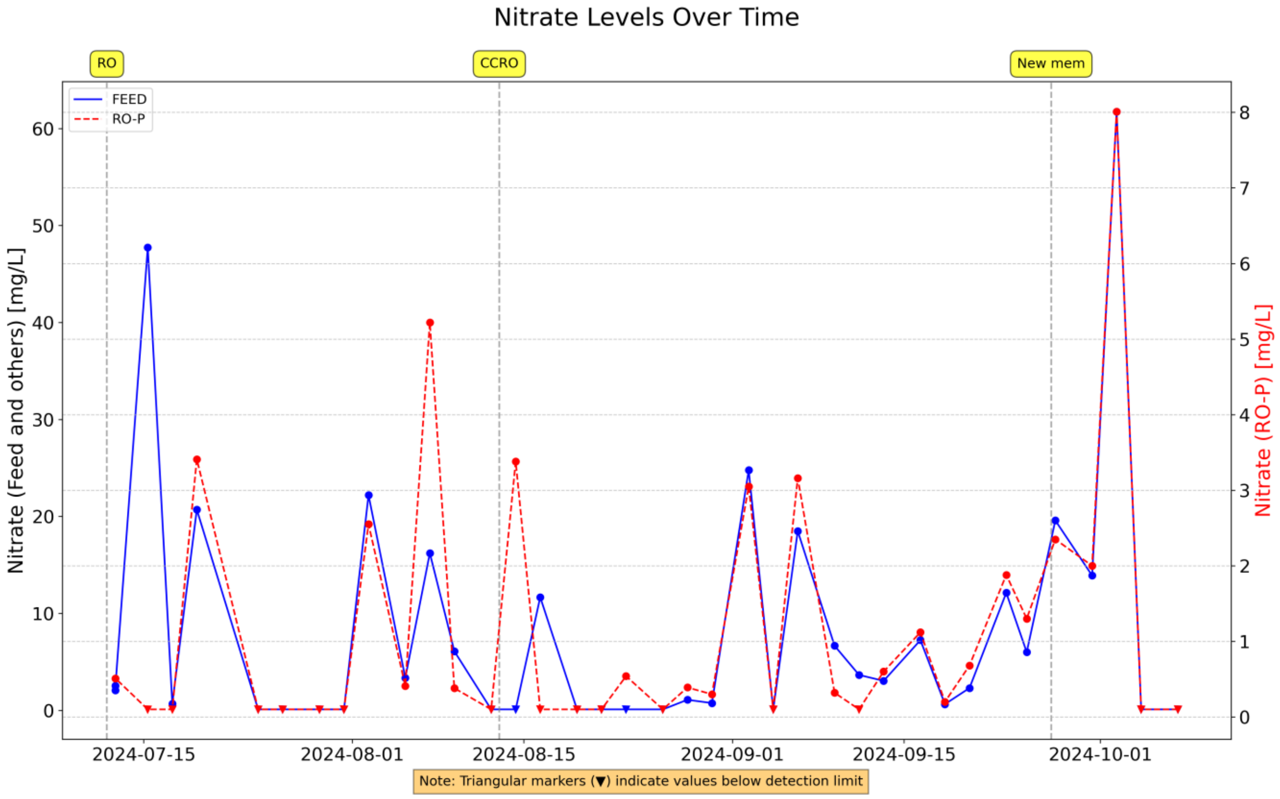

Figure 28 Nitrate levels in the feed and the RO permeate

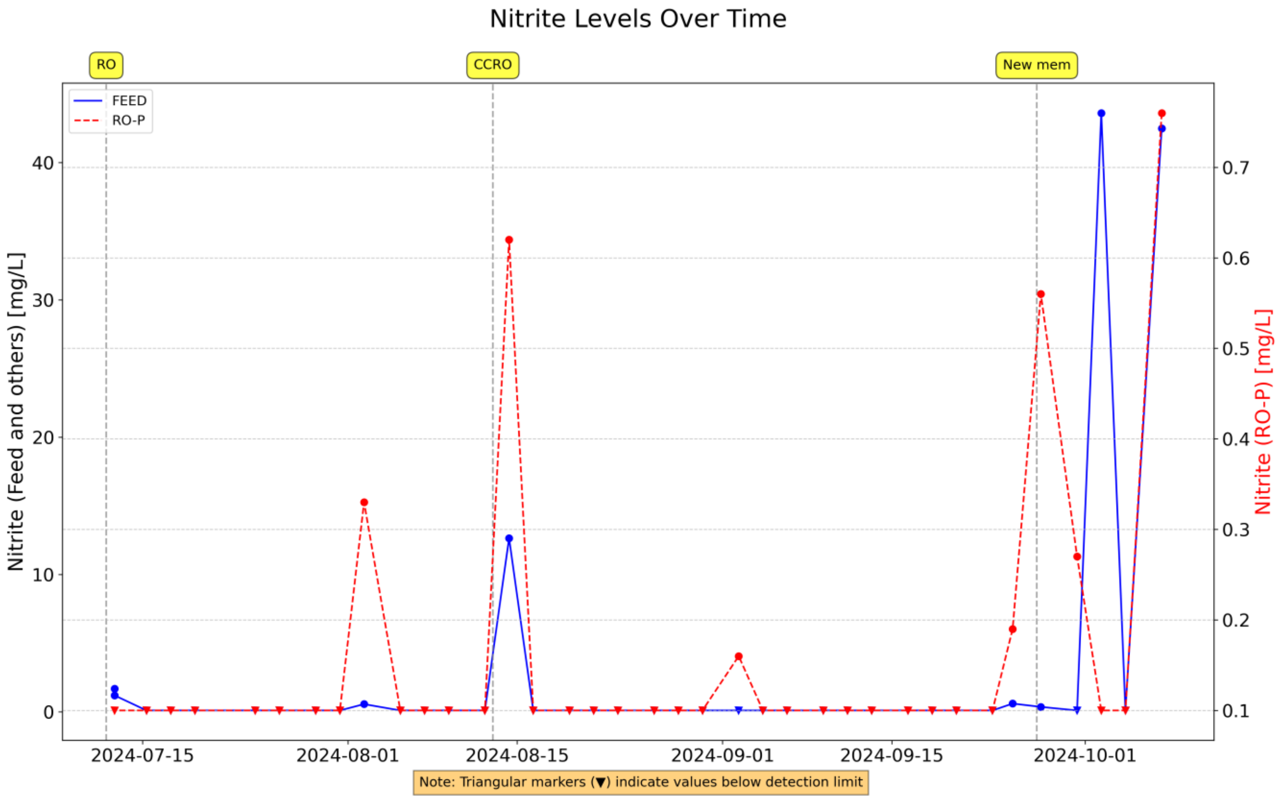

Note: Triangular markers (▼) indicate values below detection limit

Figure 29 Nitrite levels in the feed and the RO permeate

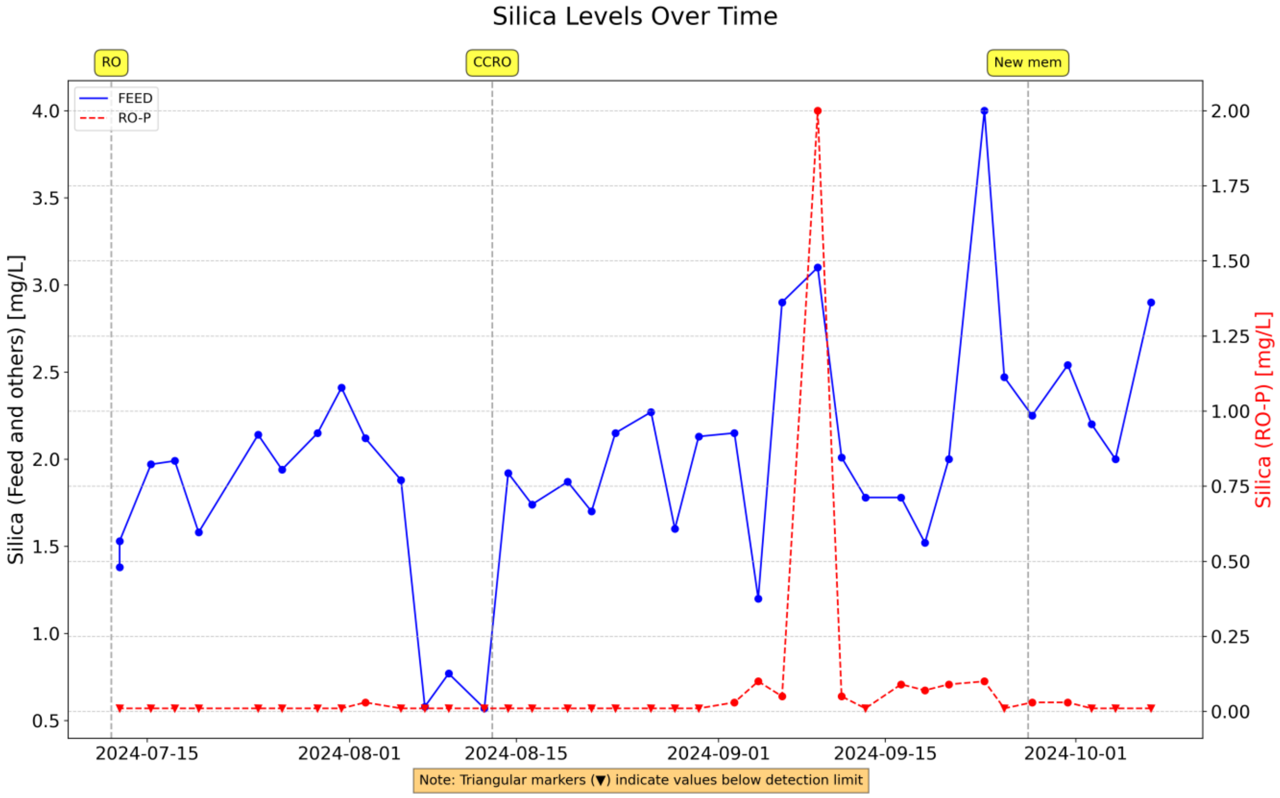

Note: Triangular markers (▼) indicate values below detection limit

Figure 30 Silica levels in the feed and RO the permeate

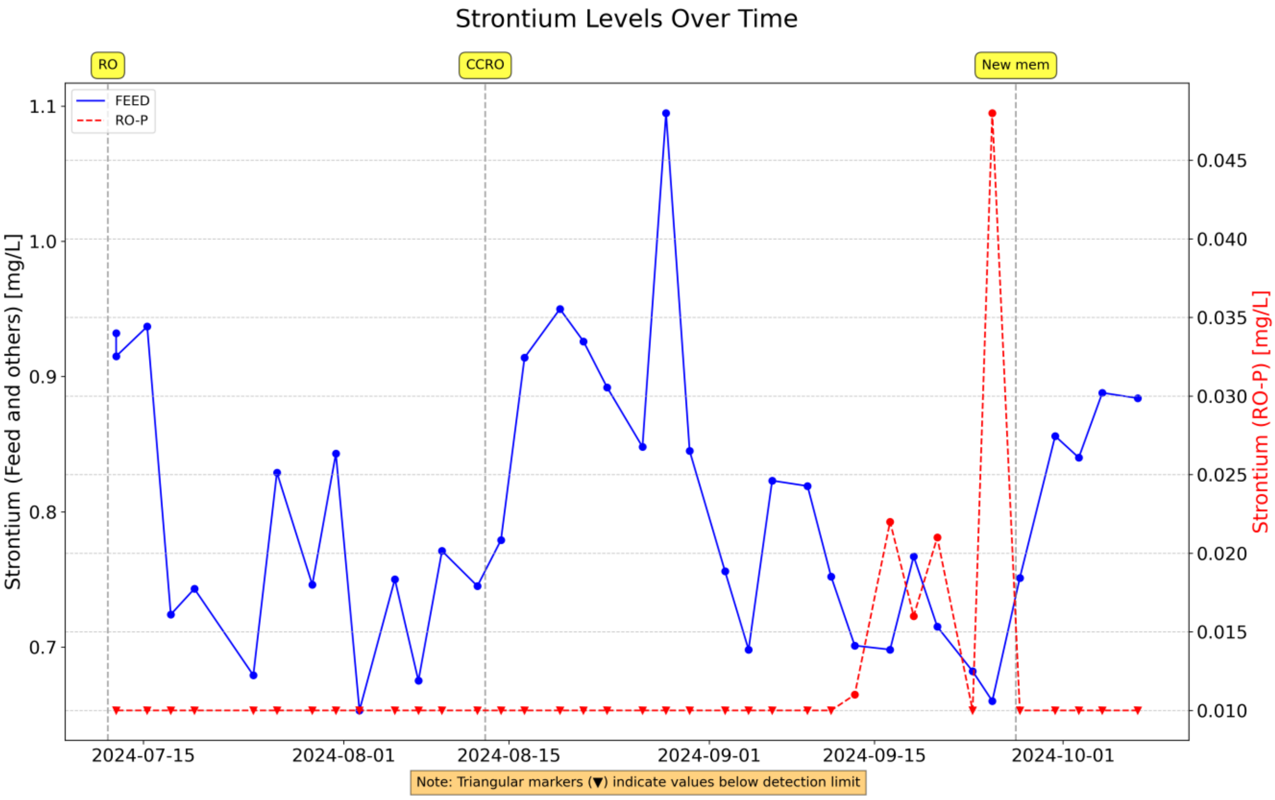

Figure 31 Strontium levels in the feed and the RO permeate

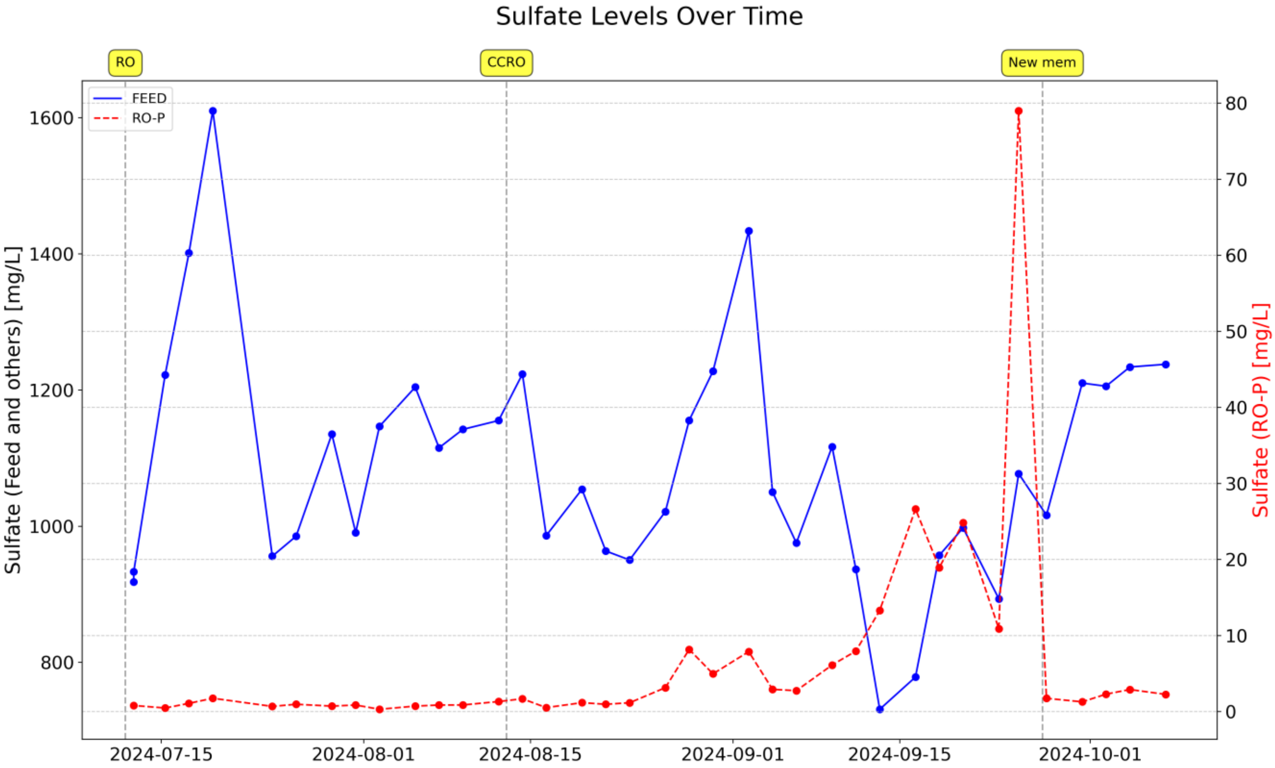

Figure 32 Sulfate levels in the feed and the RO permeate

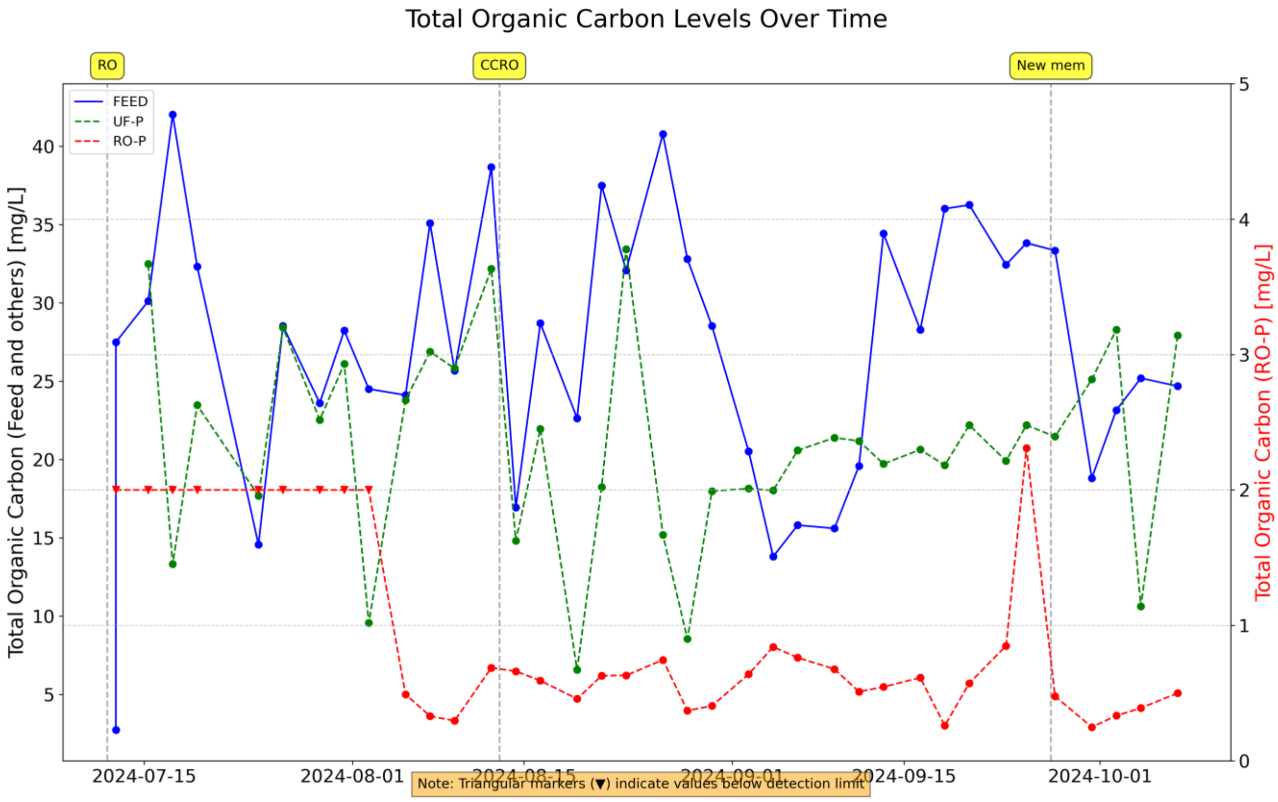

Figure 33 TOC levels in the feed and the RO permeate. Please note the higher detection limit in the beginning of the tests

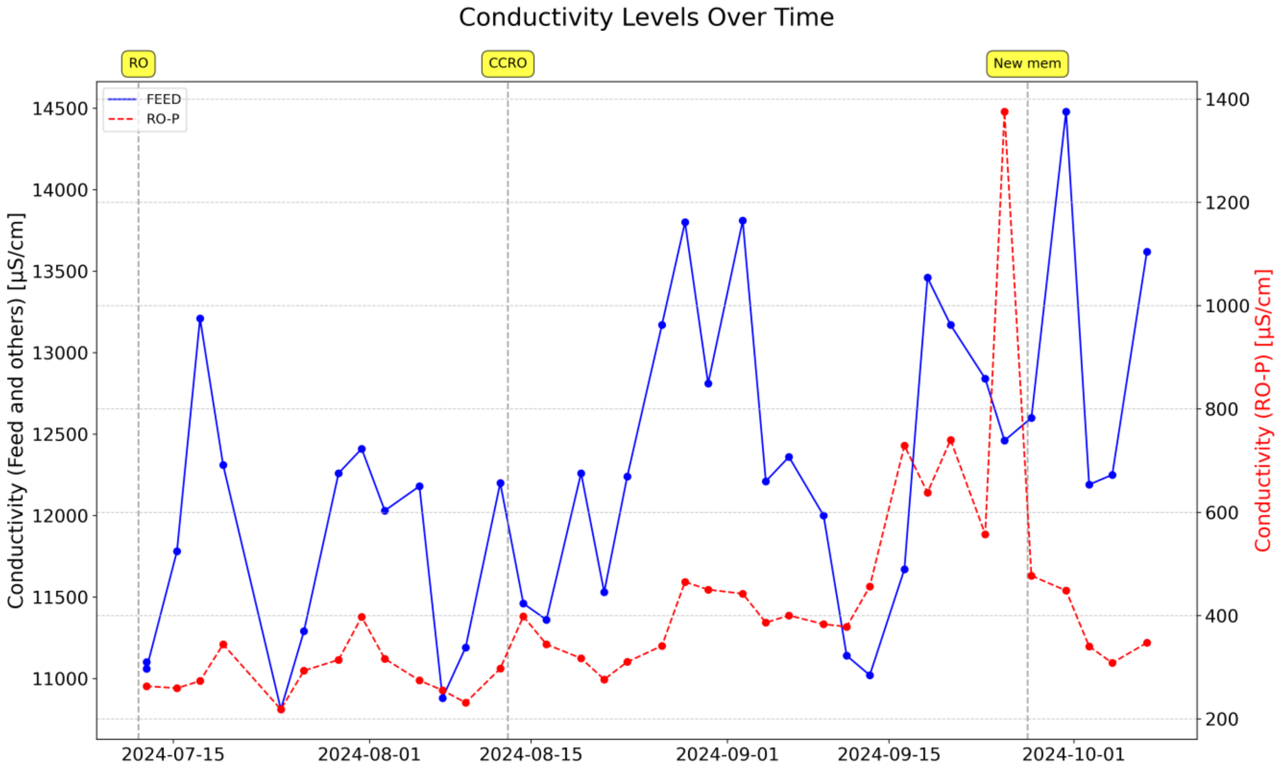

Figure 34 Conductivity of the feed and the RO permeate

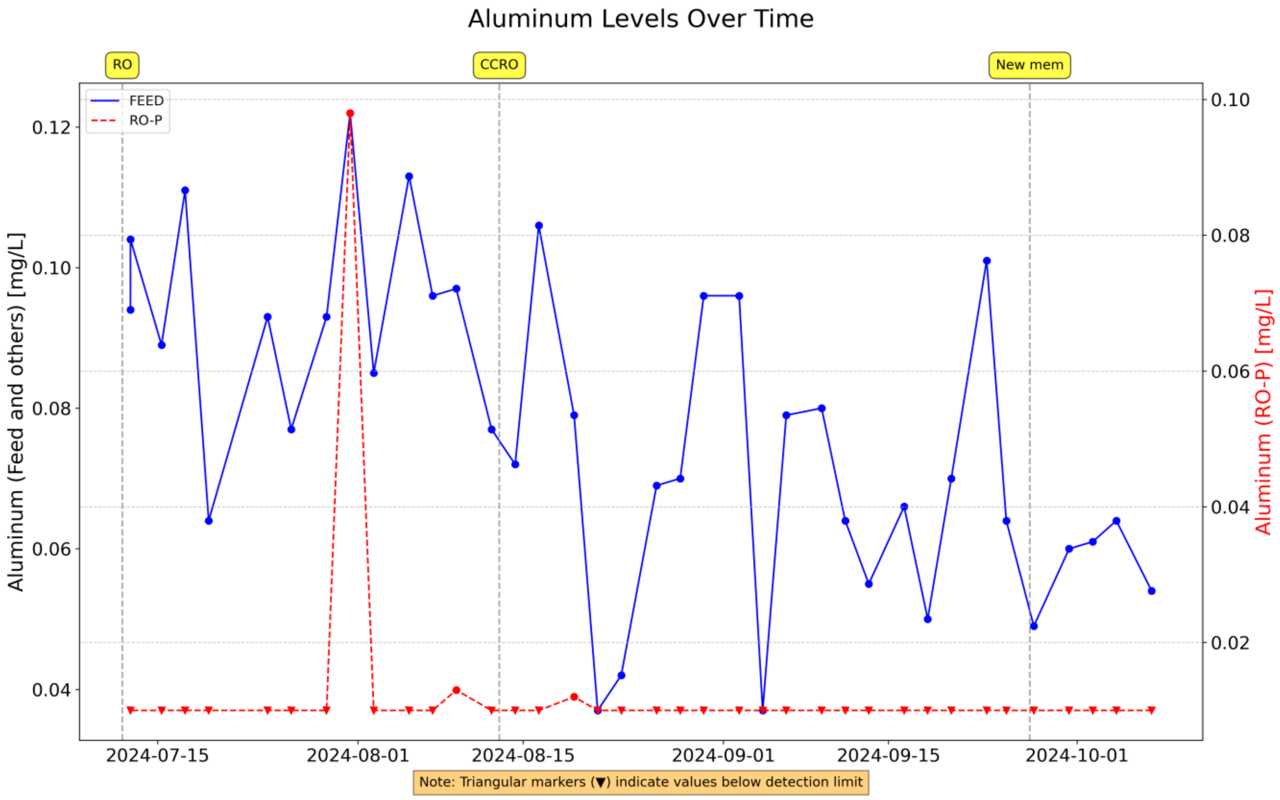

Figure 35 Aluminum levels in the feed and the RO permeate

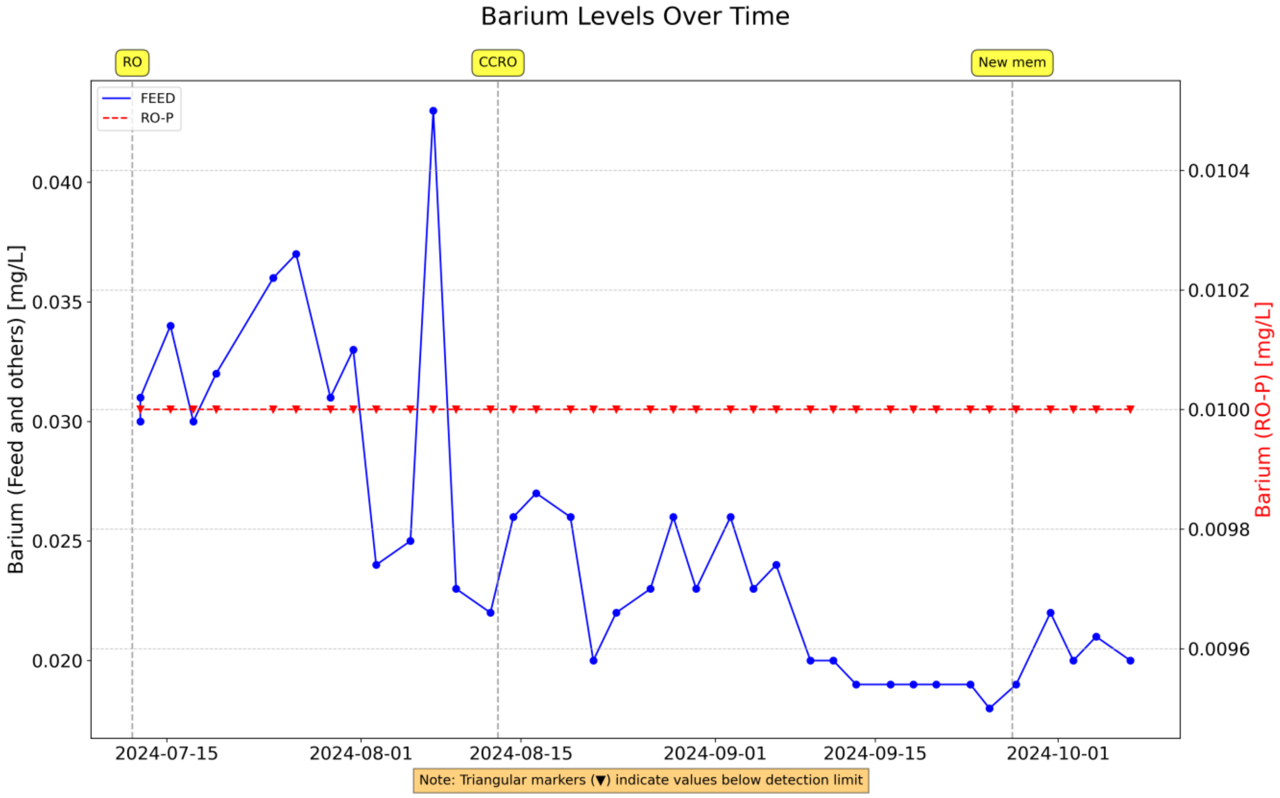

Figure 36 Barium levels in the feed and the RO permeate

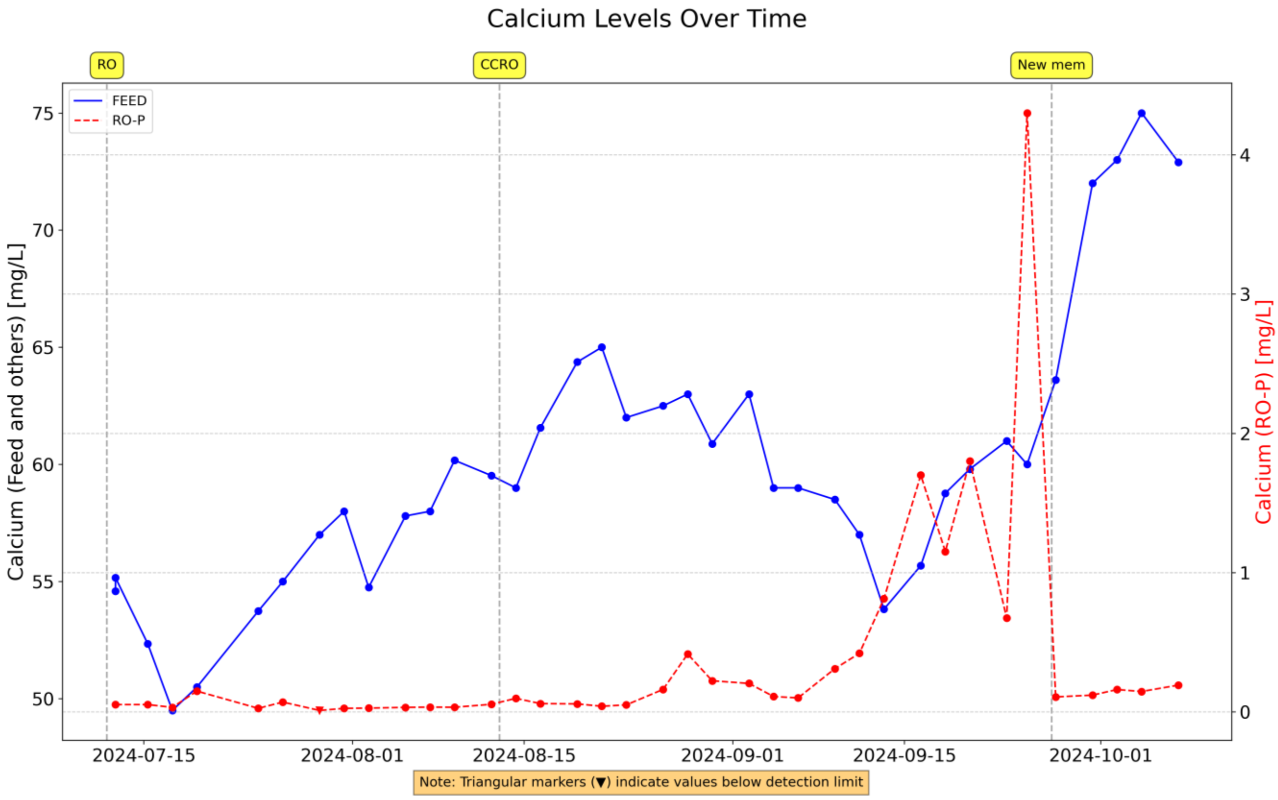

Figure 37 Calcium levels in the feed and the RO permeate

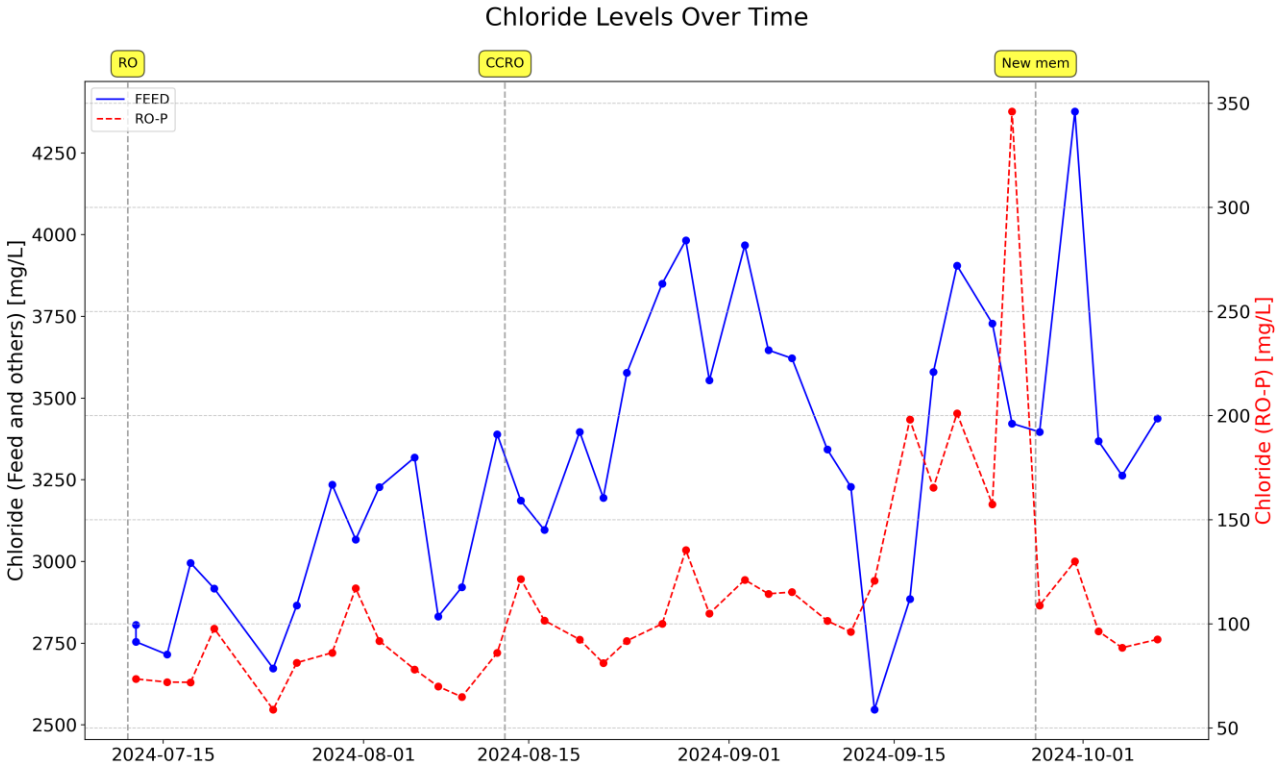

Figure 38 Chloride levels in the feed and the RO permeate

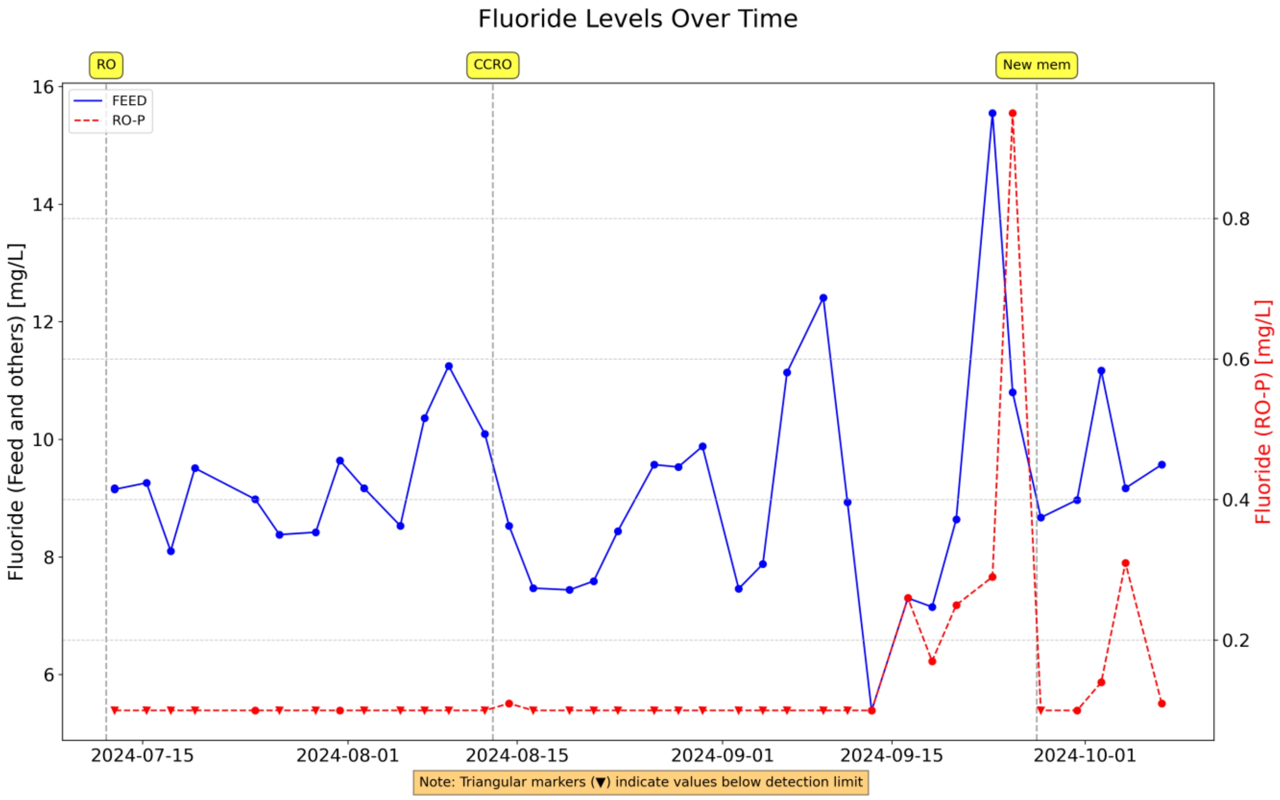

Figure 39 Fluoride levels in the feed and the RO permeate

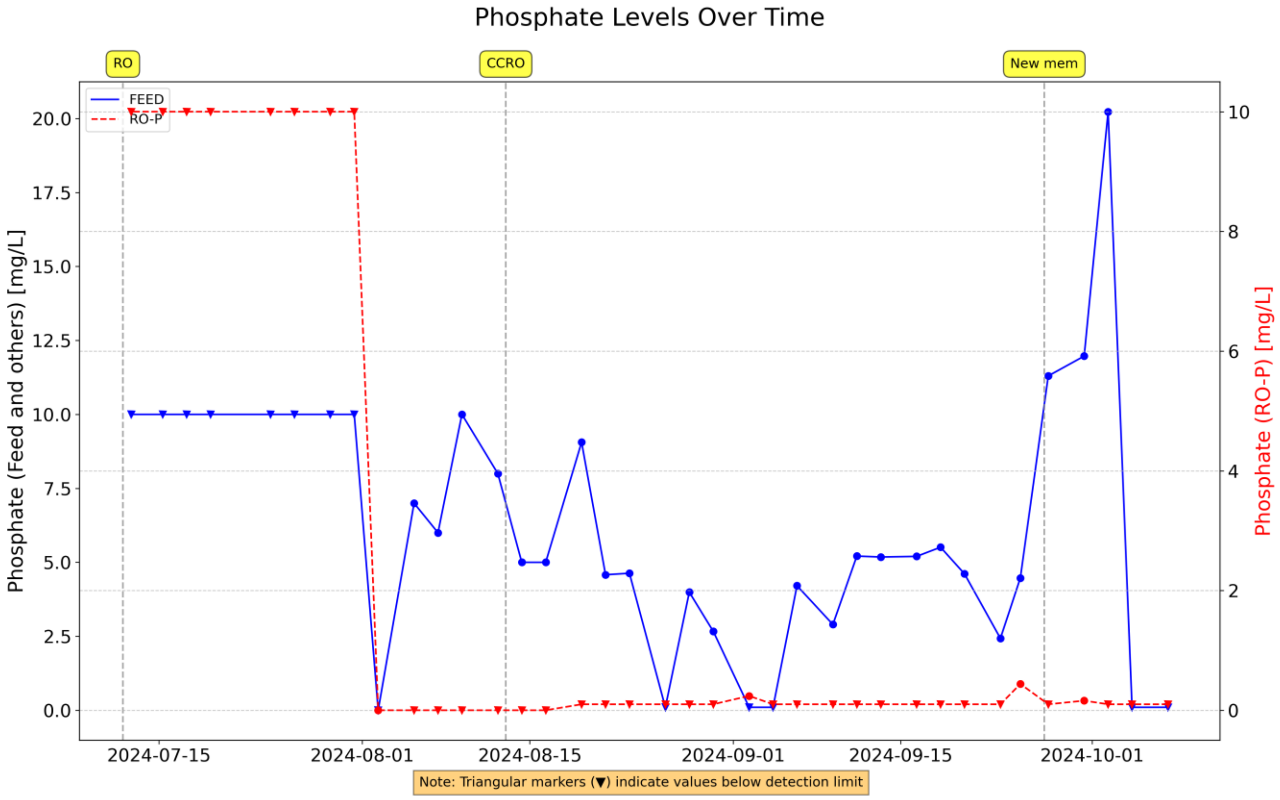

Figure 40 Phosphate levels in the feed and the RO permeate. Please note the higher detection limit in the beginning of the tests

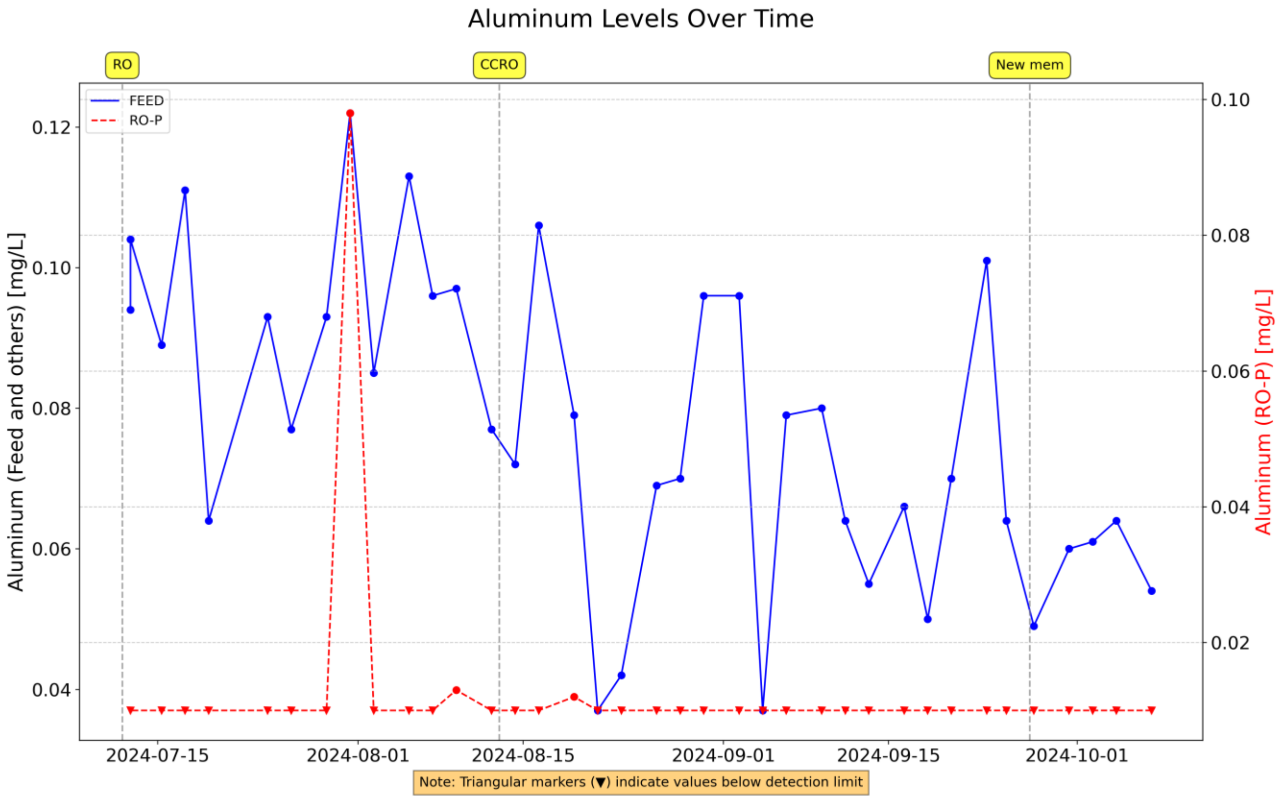

Figure 41 Aluminum levels in the feed and the RO permeate

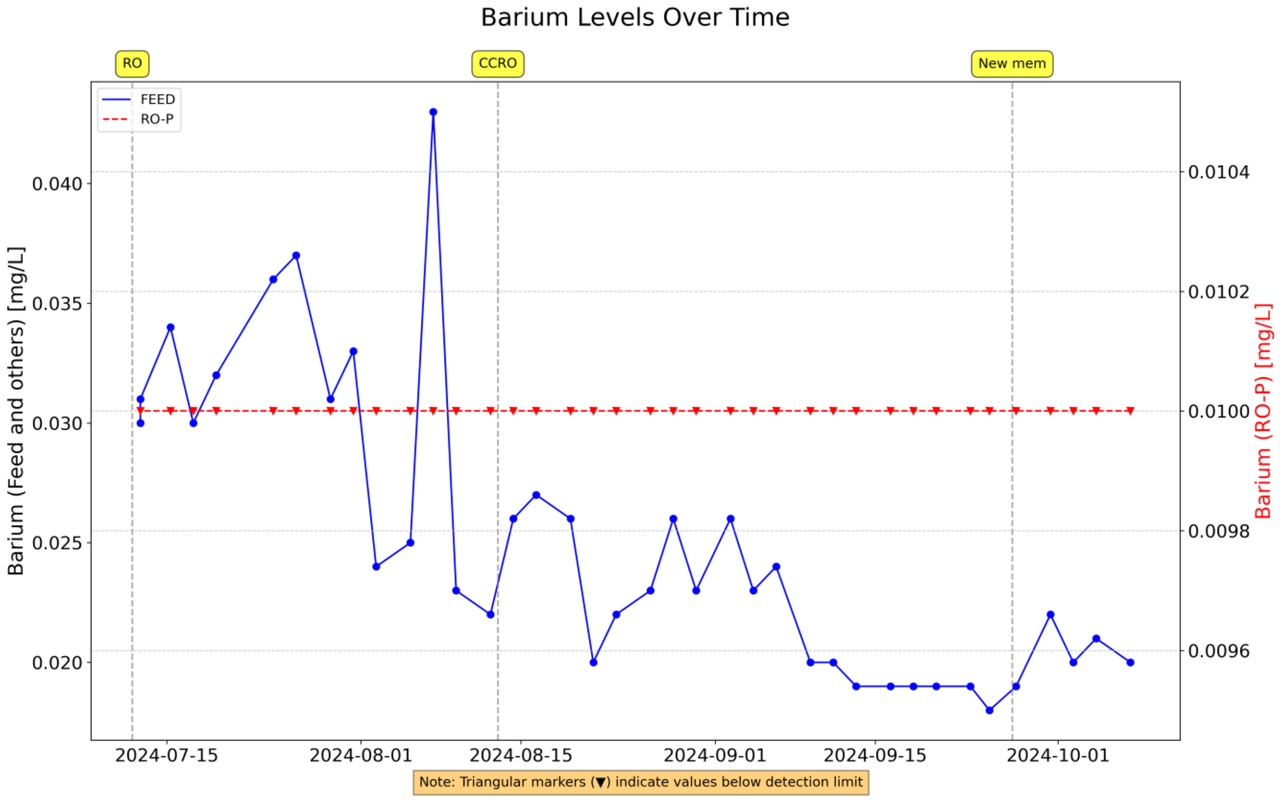

Figure 42 Barium levels in the feed and the RO permeate

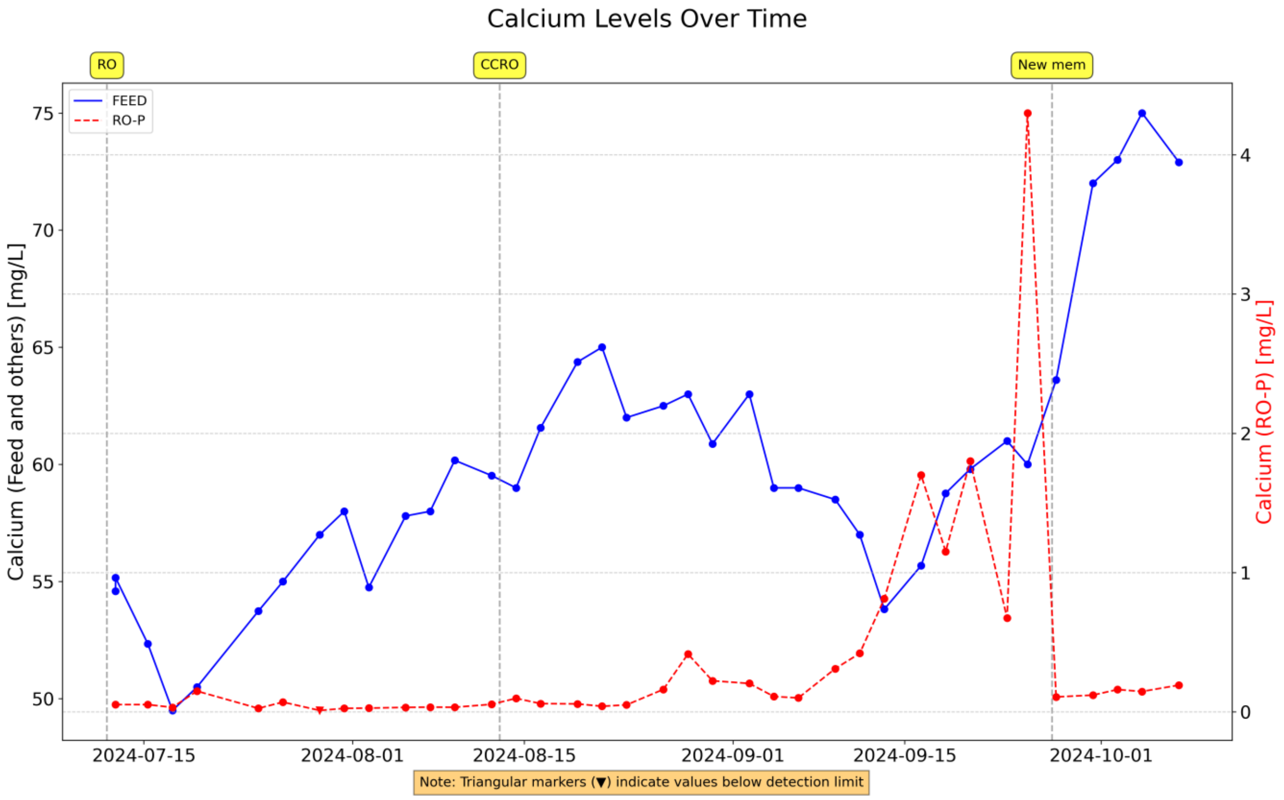

Note: Triangular markers (▼) indicate values below detection limit

Figure 43 Calcium levels in the feed and the RO permeate

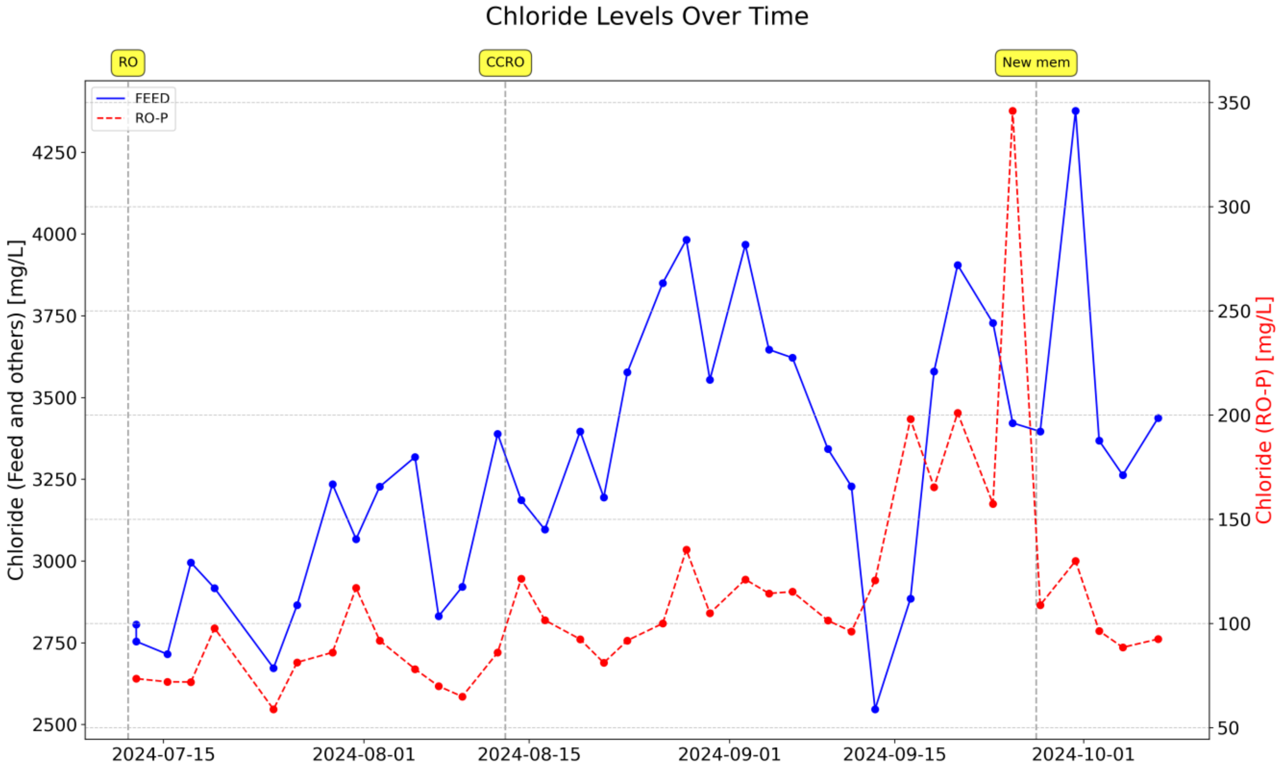

Figure 44 Chloride levels in the feed and the RO permeate

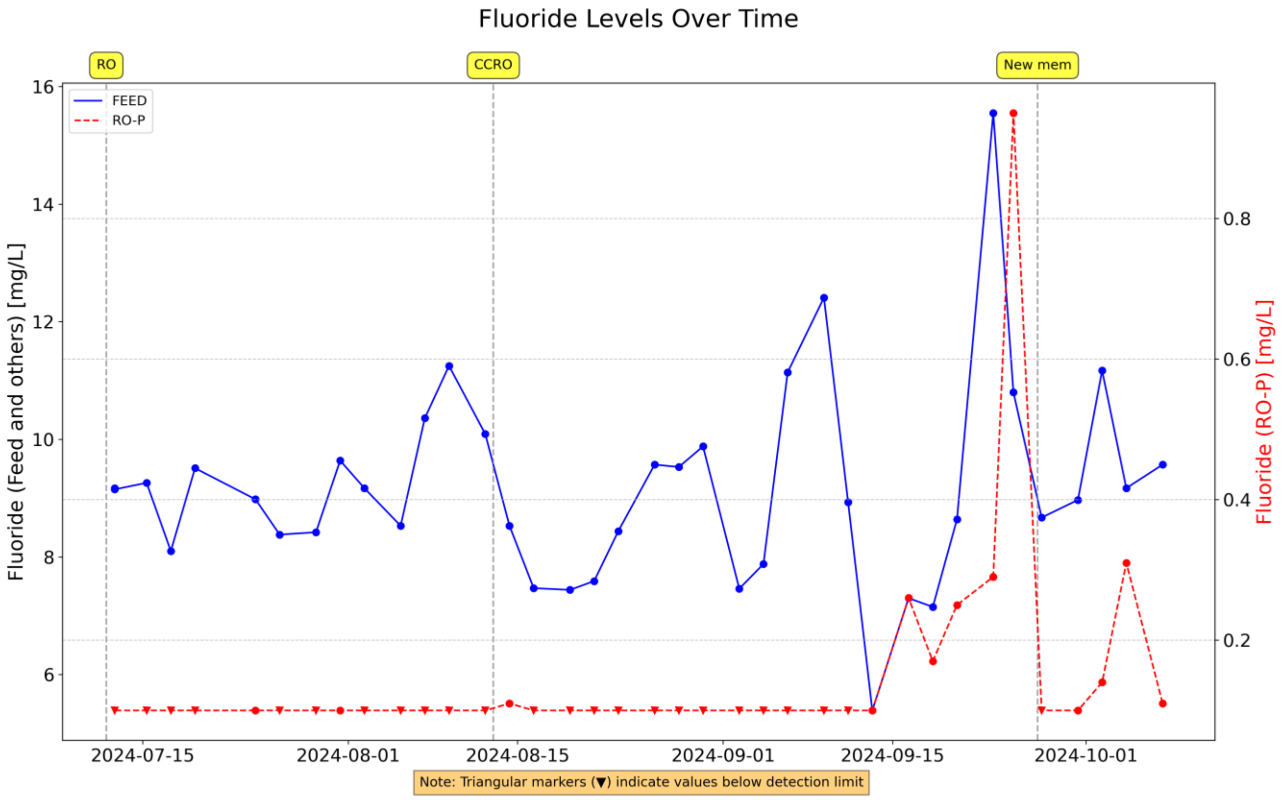

Figure 45 Fluoride levels in the feed and the RO permeate

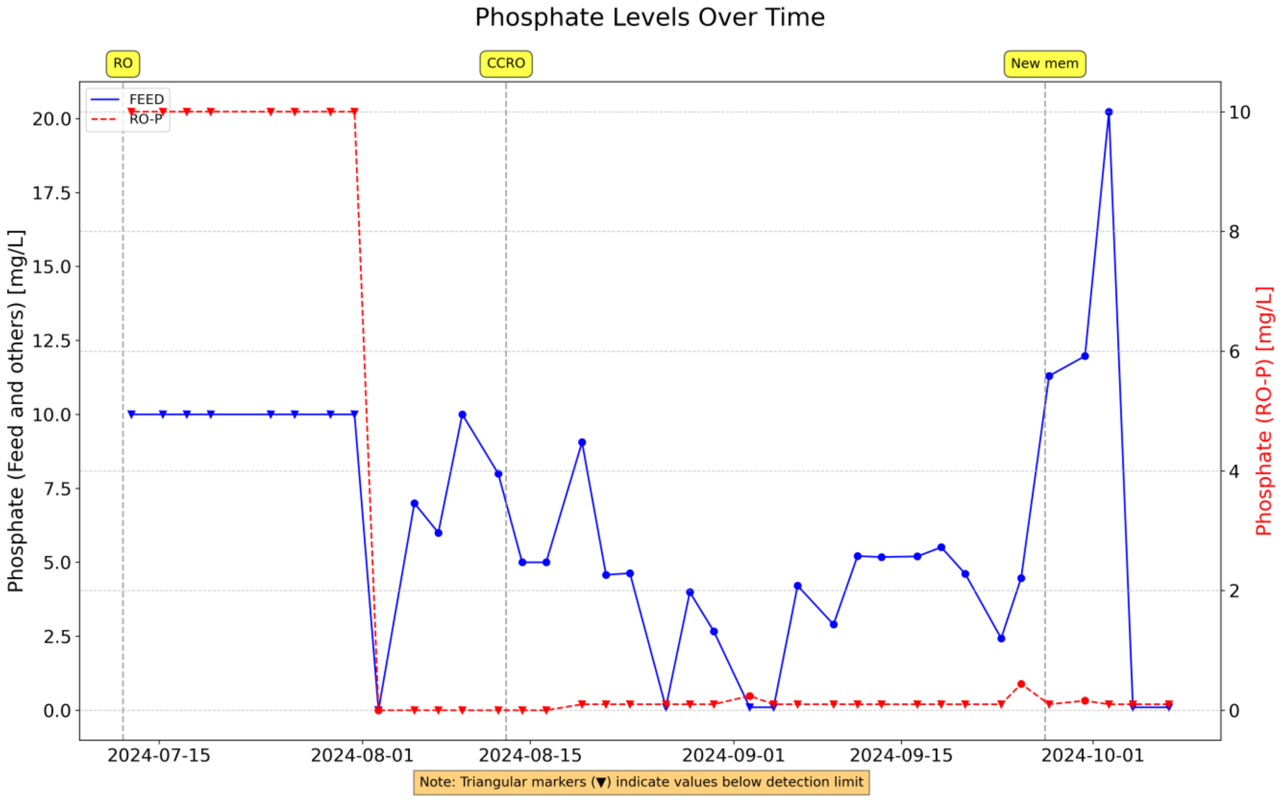

Figure 46 Phosphate levels in the feed and the RO permeate. Please note the higher detection limit in the beginning of the tests

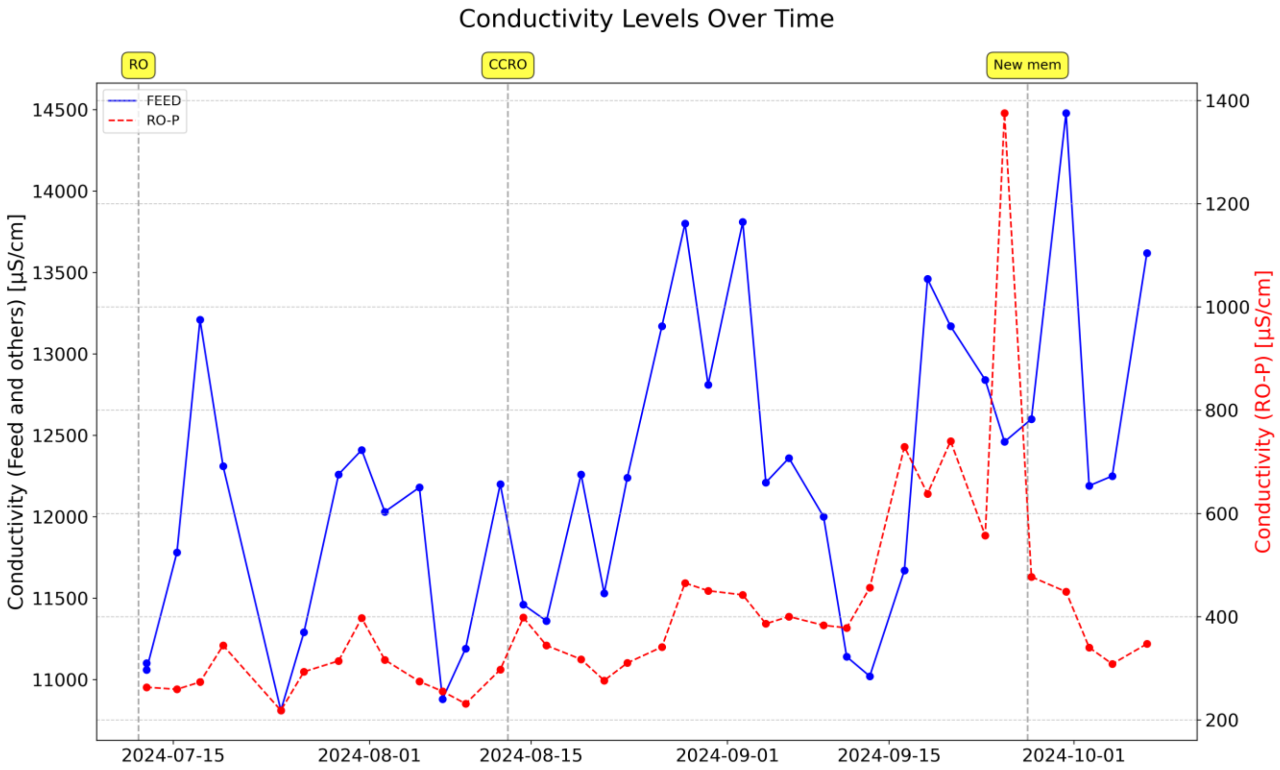

Figure 47 Conductivity of the feed and the RO permeate (Measured in grab samples in the lab)

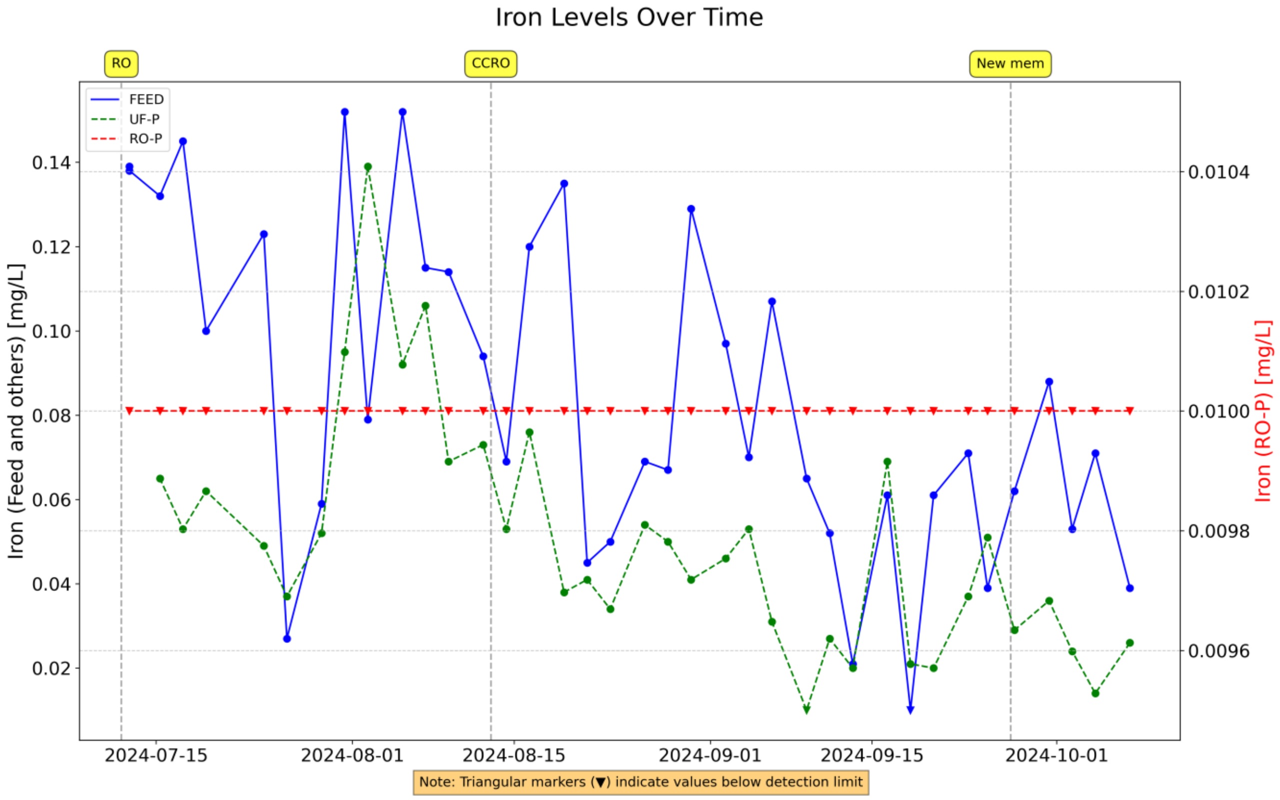

Figure 48 Iron levels in the feed and the RO permeate

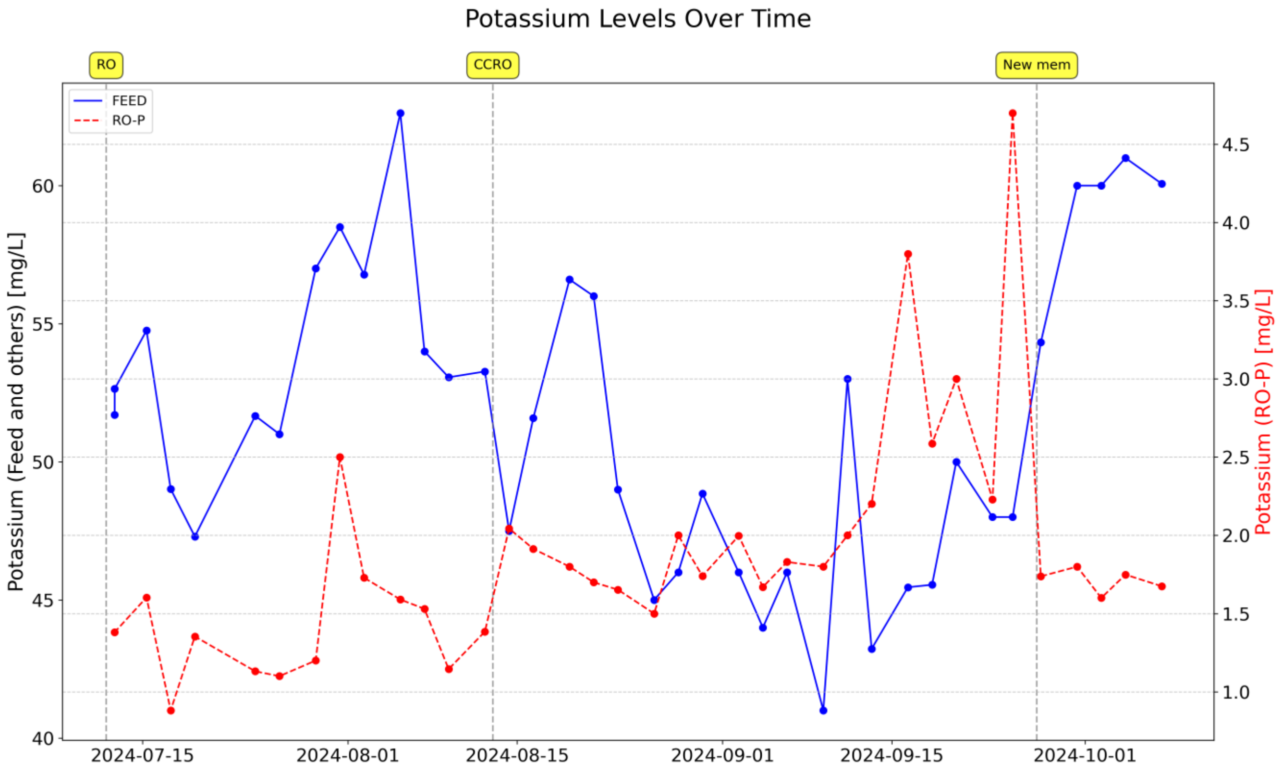

Figure 49 Potassium levels in the feed and the RO permeate

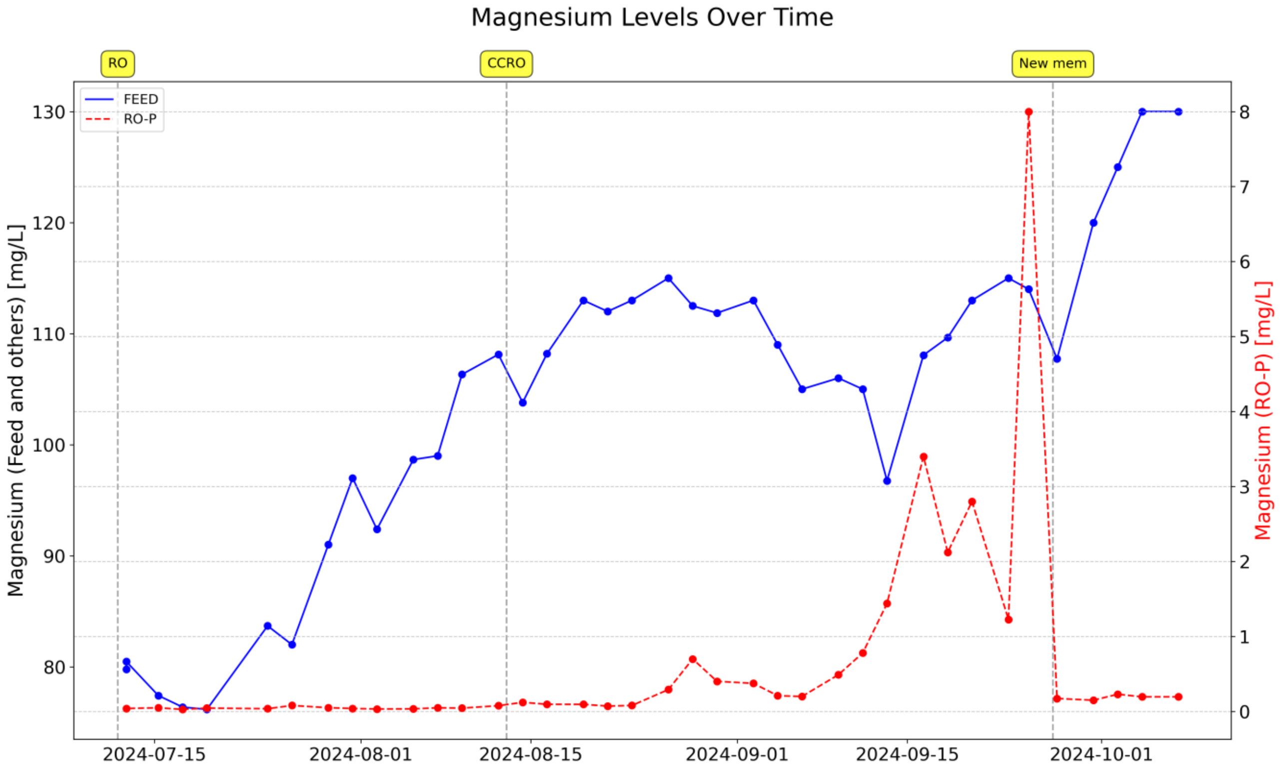

Figure 50 Magnesium levels in the feed and the RO permeate

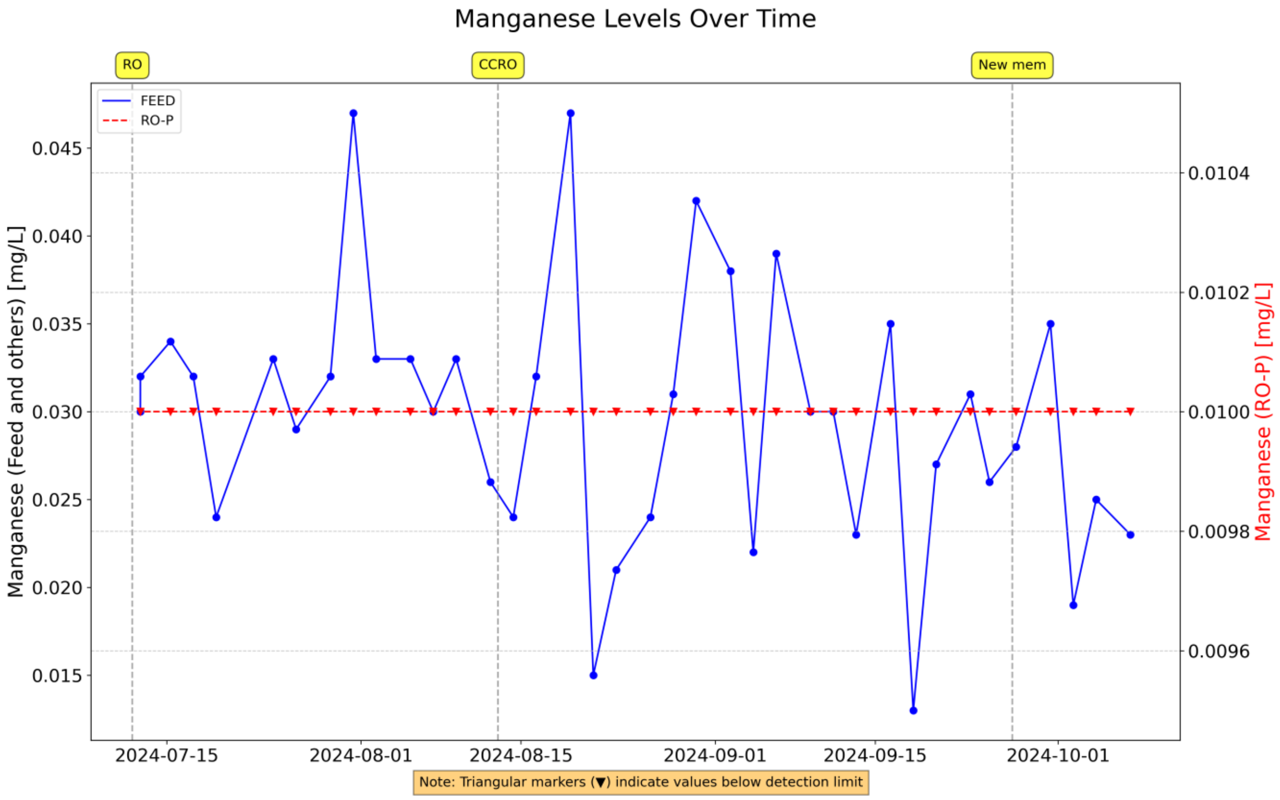

Figure 51 Manganese levels in the feed and the RO permeate

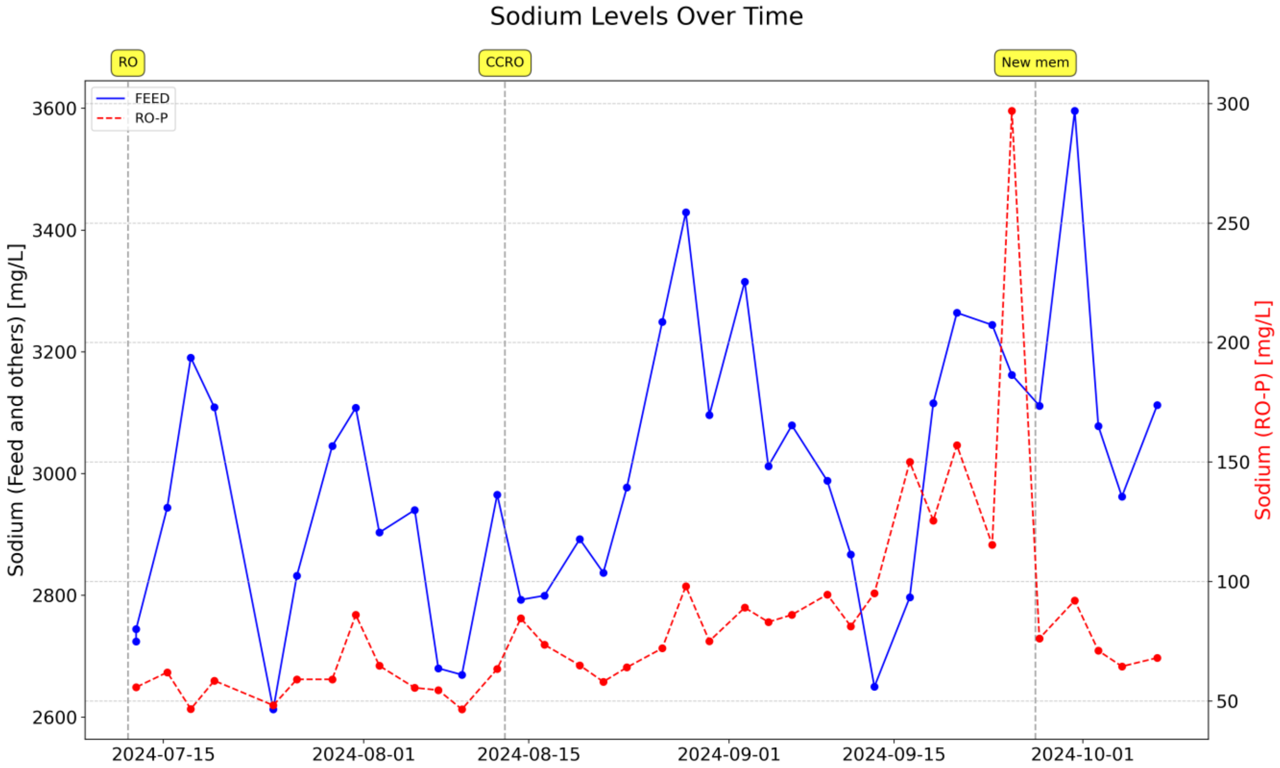

Figure 52 Sodium levels in the feed and the RO permeate